行政院國家科學委員會補助專題研究計畫成果報告

※※※※※※※※※※※※※※※※※※※※※※※※※※

※ Dipyridamole 抑制人類腹膜表面細胞增生機轉之進一步探討 ※

※ 及其在生體抑制鼠腹膜纖維化之療效 ※

※ ※

※※※※※※※※※※※※※※※※※※※※※※※※※※

計畫類別：■個別型計畫　□整合型計畫

計畫編號：NSC89－2314－B－002－507－

執行期間：89 年 8 月 1 日至 90 年 8 月 31 日

計畫主持人：蔡敦仁

共同主持人：洪冠予

本成果報告包括以下應繳交之附件：

- □赴國外出差或研習心得報告一份
- □赴大陸地區出差或研習心得報告一份
- □出席國際學術會議心得報告及發表之論文各一份
- □國際合作研究計畫國外研究報告書一份

執行單位：國立臺台灣大學醫學院內科

中　華　民　國　90 年　10　月　20　日

Kidney International, Vol. 60 (2001), pp. 872–881

Dipyridamole inhibits PDGF-stimulated human peritoneal mesothelial cell proliferation

KUAN-YU HUNG, CHIN-TIN CHEN, CHUNG-JEN YEN, PO-HUANG LEE, TUN-JUN TSAI, and BOR-SHEN HSIEH

Departments of Internal Medicine, Center for Optoelectronic Biomedicine, and Surgery, College of Medicine, National Taiwan University, Taipei, Taiwan, ROC

Dipyridamole inhibits PDGF-stimulated human peritoneal mesothelial cell proliferation.

Background. It has been proposed that proliferation of human peritoneal mesothelial cells (HPMCs) accompanied by collagen synthesis may contribute to the development of peritoneal fibrosis (PF) in patients of long-term continuous ambulatory peritoneal dialysis (CAPD). However, the precise molecular mechanism regulating HPMC proliferation has never been reported. Dipyridamole has been reported to have potential as an antiproliferative and antifibrotic agent. We investigated the mechanism and effect of dipyridamole in regulation of HPMC proliferation.

Methods. HPMCs were cultured from human omentum by an enzyme digestion method. Cell proliferation was measured by the methyltetrazolium assay and intracellular cAMP was measured using an enzyme immunoassay kit. Cell-cycle distribution of HPMC was analyzed by flow cytometry. Extracellular signal-regulated protein kinase (p44/p42 ERK) activity and expressions of cell-cycle proteins (cyclin D_1, CDK4, pRB and $p27^{Kip1}$) were determined by Western blotting.

Results. The addition of DP suppressed PDGF-stimulated HPMC proliferation by cell-cycle arrest at the G_1 phase. The antimitogenic effect of dipyridamole was mediated through the cAMP pathway. PDGF (25 ng/mL) increased the ERK1/2 activity of HPMC within 15 minutes, which maximized at 30 minutes, and the pretreatment with dipyridamole (17 μg/mL) substantially reduced the ERK response to PDGF by approximately 78.5%. PDGF induced elevated protein levels of cyclin D_1, but the CDK4 protein level did not change. Dipyridamole and DBcAMP had no effect on the levels of cyclin D_1 and CDK4 in PDGF-stimulated HPMC. PDGF decreased $p27^{Kip1}$ and induced pRB phosphorylation of HPMC. In contrast, dipyridamole prevented PDGF-induced $p27^{Kip1}$ degradation and attenuated PDGF-stimulated pRB phosphorylation.

Conclusion. Dipyridamole appears to inhibit PDGF-stimulated HPMC proliferation through attenuated ERK activity, preservation of $p27^{Kip1}$, and decreased pRB phosphorylation. Thus, dipyridamole may have therapeutic efficacy to prevent or alleviate PF.

Key words: extracellular protein kinase cascade, dipyridamole, fibrosis, cell signaling, $p27^{Kip1}$, signal transduction.

Received for publication June 20, 2000
and in revised form March 22, 2001
Accepted for publication March 26, 2001

The successful use of peritoneal dialysis (PD) as a long-term replacement therapy depends on the sustained integrity of the peritoneal membrane. Peritoneal fibrosis (PF), a serious complication found occasionally in patients on long-term PD, has been demonstrated to compromise the peritoneal membrane to a severe degree [1, 2]. Research examining the mechanisms underlying PF has shown that proliferation of human peritoneal mesothelial cells (HPMCs) accompanied by collagen synthesis play a certain role in the pathogenesis of PF [1, 2]. However, the precise cellular mechanism regulating HPMC proliferation has, to our knowledge, never been reported.

Platelet-derived growth factor (PDGF) has been reported to be elevated during peritoneal injury [3]. In rat pleural mesothelial cell culture, PDGF has been shown to stimulate PMC proliferation and collagen synthesis [4]. The extracellular signal-regulated protein kinase (ERK), namely, the ERK1/2 (p44/p42) cascade, is considered to play a critical role in the downstream signals of PDGF [5]. In both human [6–8] and rat [9] aortic smooth muscle cells (SMC), PDGF stimulates the sustained activation of ERK consistent with a role in cellular proliferation as well as initiating DNA synthesis. Furthermore, it has been shown that abrogation of ERK expression activation using antisense approaches abolishes PDGF-stimulated DNA synthesis in SMC [10] as well as in fibroblasts [11]. Thus, in PF where accelerated HPMC proliferation is a feature, strategies designed to inhibit the PDGF-stimulated ERK activation of HPMC may be clinically relevant to the prevention or retardation of PF.

Dipyridamole [2,6-bis(diethanolamino)-4,8-dipiperidinopyrimido-(5,4-d)-yrimidine] is used as an antiplatelet agent [12]. In addition to its antiplatelet activity, it has been shown to exert antiproliferative effects on human vascular SMC [8], human mesangial cells [13], and rat

mesangial cells [14]. Dipyridamole has been well documented to act as a phosphodiesterase inhibitor that increases intracellular cAMP [12, 13]. In rat aortic SMC [9] and mesangial cells [15] it has been shown that raising intracellular cAMP results in the inhibition of agonist-stimulated ERK. Our previous report demonstrated that dipyridamole, through increased intracellular cAMP, may inhibit rat mesangial cell proliferation and reduce the expression of collagen α1(I) mRNA [14]. However, its mechanism remains undetermined.

Cell proliferation is governed by the cell-cycle machinery. In mammalian cells, progression through the cell cycle is dependent on the balance of positive and negative regulatory cell-cycle proteins [16]. Cyclin D_1 plays a vital role in G_1 phase progression. Cyclin D_1, when bound to its catalytic partner, the cyclin-dependent kinase 4 (CDK4), may result in the formation of active cyclin D_1/CDK4 complex, which is responsible for the phosphorylation of the retinoblastoma gene product (pRB). Unphosphorylated pRB negatively controls G_1 progression, and the phosphorylated form of pRB is essential and required for proliferation of normal cells [17, 18]. Cyclin-kinase inhibitors (CKIs) negatively regulate the cell cycle by inhibiting the cyclin D_1/CDK4 complex. $p27^{Kip1}$ is regarded as a major CKI of the G_1 phase and is most directly involved in cell cycle restriction control [19, 20]. In quiescent Balb/c-3T3 cells, the $p27^{Kip1}$ level is high and the cell cycle stops in G_1 phase [19]. A reduction of $p27^{Kip1}$ expression by PDGF results in cell-cycle re-entry and proliferation of rat mesangial cells [20]. While cyclins and CDKs have been well investigated in a wide range of mammalian cell types, there has been, to our knowledge, no report detailing their induction and regulation in HPMCs.

Our current study found that dipyridamole arrested HPMC at the G_1 phase. Furthermore, we identified the ERK cascade and determined the expression of cell-cycle regulatory proteins in HPMCs. Our data show that dipyridamole inhibited PDGF-stimulated HPMC proliferation mainly through attenuated ERK activity and alterations of cell-cycle proteins.

METHODS

Materials

Fetal calf serum (FCS) was obtained from Biochrome KG (Berlin, Germany). Culture flasks and plates were purchased from Corning (Corning, NY, USA) and precoated with 1.6 μg/cm² of Vitrogen 100® (Celtrix Lab, Palo Alto, CA, USA) before cell loading. Trypsin-EDTA, RPMI-1640 medium, glutamine, and trypan blue were obtained from GIBCO (Grand Island, NY, USA). Aprotinin, adenosine 5′-triphosphate (ATP), leupeptin, phenylmethylsulfonyl fluoride (PMSF), sodium orthovanadate (Na_3VO_4), bovine serum albumin (BSA), 3-[4,5-dimethylthiazol-2-yl]-2,5-diphenyltetrazolium bromide (MTT), dibutyryl-cAMP (DBcAMP), 3-isobutyl-1-methylxanthine (IBMX), human recombinant PDGF-AB, and other tissue culture reagents were purchased from Sigma (St. Louis, MO, USA). The enzyme immunoassay (EIA) kits for cAMP were obtained from Cayman Chemical (Ann Arbor, MI, USA). Selective cAMP-dependent protein kinase (PKA) inhibitor, H-89, was obtained from Calbiochem (La Jolla, CA, USA). Bicinchoinic acid (BCA) reagents were obtained from Pierce (Rockford, IL, USA). Anti-phospho-ERK1/2 and anti-ERK1/2 were purchased from New England Biolabs (Beverly, MA, USA). Anti-CDK4, anti-cyclin D_1, anti-pRB, and anti-$p27^{Kip1}$ antibodies were obtained from Santa Cruz Biotechnology (Santa Cruz, CA, USA). Dipyridamole was generously provided by Boehringer Ingelheim. All other chemicals used were of analytical grade.

Establishment of human PMC culture

Specimens of human omentum were obtained from abdominal surgical procedures for elective gastric cancer resection and the omentum was grossly inspected as normal. The HPMC culture was performed as previously reported [21, 22]. Briefly, the surgically removed human omentum was washed three times with PBS and then digested with trypsin ethylenediaminetetraacetic acid (EDTA; 0.125%; GIBCO) for 15 minutes. After centrifugation, the cell pellet was washed with culture medium and then seeded into a gelatin-coated (1 mg/mL) flask. Medium was changed on the third day. RPMI-1640 medium containing 20% FCS, penicillin (100 U/mL), streptomycin (100 μg/mL), and insulin (30 μg /mL) was used. After two to four days, the cells became confluent and were subcultured with medium containing 10% FCS. HPMCs were identified by the presence of vimentin and cytokeratin, but without desmin and factor VIII-related antigen, by the immunoflurescence method. All experiments were performed in passage 1–3 cells.

Cell proliferation assay

A modified MTT assay was used to evaluate HPMC proliferation as previously reported [14, 21, 22]. The amount of MTT uptake (absorbance at 570 nm) by HPMC was found to vary linearly with cell numbers ranging from 4000 cells/well to 12.8×10^4 cells/well were loaded in 96-well plates. Therefore, 5000 cells/well for each MTT assay. Cells growing in log phase were trypsinized and plated down in 96-well plates with RPMI-1640 medium containing 10% FCS. Various concentrations of treatment agents were added after overnight plating. The medium and drug were changed every three days. After additional incubations of 24 to 120 hours, 20 μL MTT solutions (5 mg/mL in PBS) were added to the culture medium. Cells were further incubated at 37°C for four hours, and then the medium was replaced by

100 μL ethanol. Absorbance at the reference wavelength of 630 nm and test wavelength of 570 nm was measured by an ELISA reader. All experiments were repeated five times. The inhibition of HPMC growth was calculated as follows [21, 22]: percentage of inhibition = 1 − [absorbance of (test well − initial plating)/absorbance of (control − initial plating)] × 100%.

Intracellular cAMP assay

Three × 10^5 HPMCs/well were loaded into a six-well plate with RPMI-1640 medium containing 10% FCS. After cells became subconfluent, they were washed twice with warm RPMI-1640 medium and then mixed with various concentrations of agents. After five minutes of incubation, the supernatants were discarded and ice-cold 95% methanol was added to each well. After 30 minutes of incubation at 4°C, the supernatants evaporated and cAMP was measured using EIA kits. The cells in wells were lysed by 0.1 mol/L NaOH, and protein content was measured by a bicinchoninic acid assay, using BSA as the standard [23].

Flow cytometric analysis of cell cycle

Six × 10^5 HPMCs were seeded into 10 cm diameter dishes and growth-arrested by 0.5% FCS for 48 hours. Flow cytometry analysis of cell-cycle distribution of HPMCs was performed 24 hours after treatment with the indicated conditions. Briefly, cells were washed twice with PBS, harvested by trypsinization, centrifuged, and resuspended with 1 mL cold PBS, and then fixed in methanol for 30 minutes on ice. After two washes with PBS, approximately 10^6 fixed cells were incubated in 1 mg/mL RNase (Calbiochem, San Diego, CA, USA) at 37°C for 30 minutes, followed by staining of the DNA with 1 μg/μL propidium iodide (Sigma) at 4°C for 30 minutes in the dark; 10^5 cells of each sample were analyzed with a Coulter EPICS 753 flow cytometer, and the percentages of cells within the G_1, S, and G_2/M phases of the cell cycle were determined [24].

Cell preparations and protein extraction

Human peritoneal mesothelial cells were grown in 10 cm dishes until subconfluent, growth-arrested for 48 hours with medium containing 0.5% FCS and then treated. After treatment, HPMCs were harvested at indicated time points with 200 μL ice-cold lysis buffer (50 mmol/L Tris-HCl, pH 7.5, 150 mmol/L NaCl, 10% glycerol, 1% Triton X-100, 2 mmol/L EDTA, 2 mmol/L EGTA, 40 mmol/L β-glycerophosphate, 50 mmol/L NaF, 10 mmol/L sodium pyrophosphate, 200 μmol/L sodium orthovanadate, 10 μg leupeptin/mL, 200 units of aprotinin/mL, 1 μmol/L pepstatin A, 1 mmol/L PMSF, 100 nmol/L okadaic acid). The cell lysate was centrifuged at 14,000 rpm for 10 minutes, and the protein concentration of the supernatant was measured by a BCA protein assay (Pierce, Rockford, IL, USA).

Measurement of ERK activities

The Western blotting analysis of ERK phosphorylation was performed by using phospho-specific antibodies (New England Biolabs, Beverly, MA, USA) according to the manufacturer's protocol. Briefly, HPMCs were 0.5% FCS starved for 48 hours and then stimulated with PDGF (25 ng/mL) at different time points. For evaluating the inhibitory effect of dipyridamole on PDGF-stimulated ERK activation, we incubated HPMC with 17 μg/mL dipyridamole for 30 minutes before stimulation with 25 ng/mL PDGF for another 30 minutes and then used Western blotting. In addition, lanes of cells were treated with H89 (3 to 10 μmol/L) for 30 minutes before dipyridamole. Cell lysates (50 μg protein) were separated by SDS-PAGE (12%) and then transferred to PVDF membrane (Millipore, Bedford, MA, USA). For immunodetection, the membranes were probed with phospho-specific ERK antibody (1:1000) followed by incubation with peroxidase-conjugated secondary antibodies (1:4000). Bands were visualized with ECL system (Amersham).

Western blot analysis of cell-cycle proteins

For Western blot analysis, 50 μg total protein extract were denatured by boiling for five minutes at 100°C and then separated on a 12% SDS-PAGE gel. For detection of pRB, a 7.5% SDS-PAGE gel was used. After electrophoresis, the gels were electroblotted onto PVDF membrane (Millipore), and then stained with Coomassie blue to check for a complete protein transfer. The Ponceaus-S staining was applied to ensure that protein loading was equal. Blots were incubated in 1 × PBS containing 0.1% Tween-20 and 5% non-fat dry milk powder to block nonspecific antibody binding. This was followed by a two-hour incubation at room temperature with antibodies of either cyclin D_1, CDK4, pRB, or $p27^{Kip1}$. Controls included omitting the primary antibody or replacing the primary antibody with rabbit serum. Western blots were developed by the ECL system.

Statistical analysis

The results are expressed as mean ± SEM, unless otherwise stated. These statistical analyses were carried out using StatView IV on a personal computer. Statistical significance ($P < 0.05$) was evaluated using the Student t test or one way analysis of variance with a modified t test performed using the Bonferroni correction.

RESULTS

Dipyridamole inhibits PDGF-stimulated proliferation of HPMCs

Growth curve experiments of HPMCs in response to PDGF with or without dipyridamole were performed to evaluate the effect of dipyridamole on PDGF-stimulated

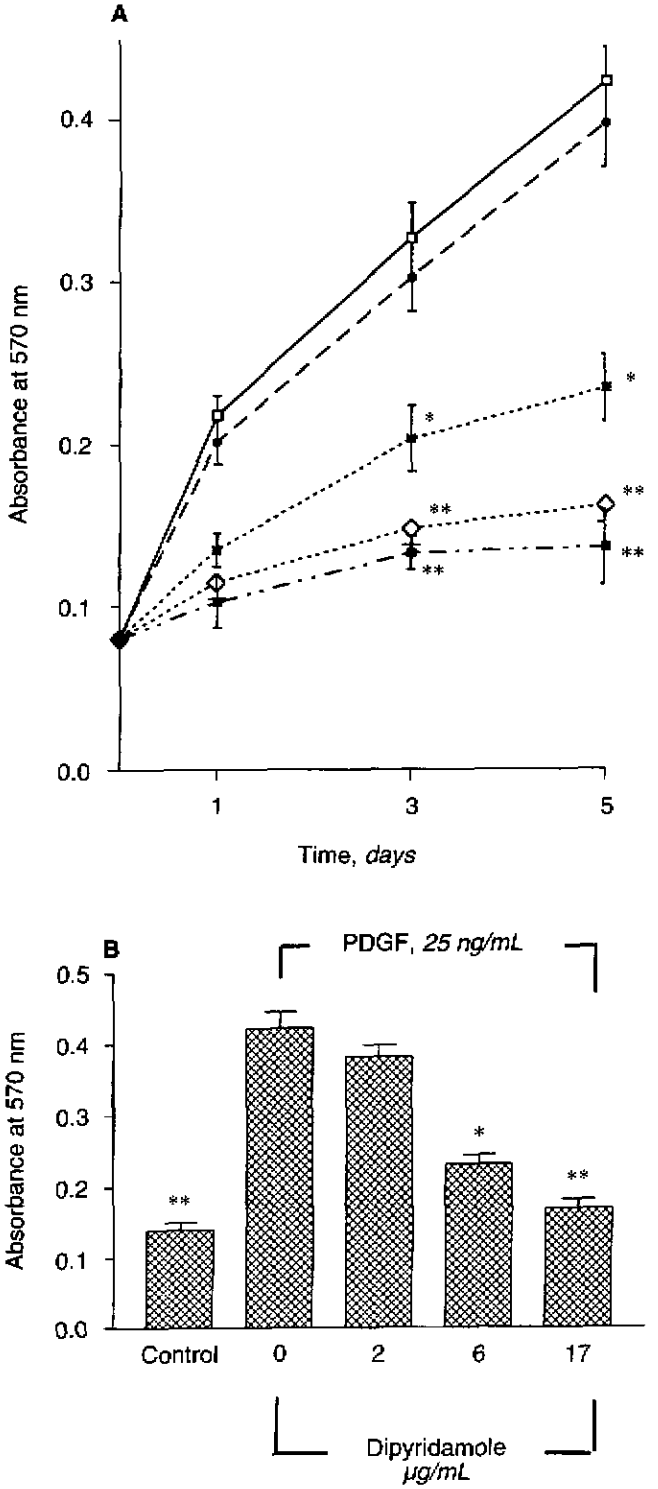

Fig. 1. Dipyridamole inhibits platelet-derived growth factor (PDGF 25 ng/mL)-stimulated human peritoneal mesothelial cell (HPMC) growth. (*A*) Time-response curve: Varying concentrations of dipyridamole were added after overnight plating of HPMC and further incubated for one to five days. Symbols are: (■) control; (□) PDGF; (●) PDGF − dipyridamole 2 μg/mL; (×) PDGF + dipyridamole 6 μg/mL; (◇) PDGF + dipyridamole 17 μg/mL. (*B*) Dose-response study: HPMCs were incubated for 120 hours after addition of varying concentrations of dipyridamole and a fixed dosage (25 ng/mL) of PDGF. $^*P < 0.05$, $^{**}P < 0.01$, compared with PDGF. Each point represents the mean ± SEM of three experiments performed in triplicate.

HPMC proliferation (Fig. 1). As expected, the addition of PDGF at a dosage of 25 ng/mL resulted in a significant increase of HPMC proliferation compared with that of unstimulated cells. This effect was clearly reduced by pretreating the cells with dipyridamole before the addition of PDGF. In time-response experiments, varying concentrations of dipyridamole were added 30 minutes before the addition of PDGF (25 ng/mL) for 24 to 120 hours. At concentrations above 6 μg/mL, dipyridamole resulted in a dose-dependent inhibition of HPMC (Fig. 1A). The dose-response effects of dipyridamole on HPMC proliferation is shown in Figure 1B. Cells were incubated for 120 hours after adding varying concentrations of dipyridamole and a fixed dose (25 ng/mL) of PDGF. When compared with the effect of PDGF alone, significant inhibition of HPMC proliferation was observed at ≥6 μg/mL dipyridamole. Dipyridamole, at concentrations of 6 μg/mL and 17 μg/mL, inhibited PDGF-stimulated HPMC proliferation by 40.1 and 57.0%, respectively. Therefore, a higher concentration of dipyridamole (17 μg/mL) was in the following experiments to show its effects on ERK cascade and cell-cycle progressions of HPMC.

To exclude the potentially toxic effect of such a concentration of dipyridamole on proliferative HPMC, cell viability tests were performed by the trypan blue exclusion method and by measuring the lactate dehydrogenase (LDH) activity of the supernatant as we previously described [21, 22]. No differences in numbers of dead cells in supernatant and adherent HPMC fractions were found between the control and dipyridamole-treated wells. The levels of LDH did not increase after one- to five-day incubation periods in the dipyridamole-treated wells, which excluded the cell membrane damage on HPMC by dipyridamole (data not shown).

Dipyridamole-induced cell-cycle arrest of HPMC at the G_1 phase

To investigate the cellular mechanism of this inhibitory effect of dipyridamole on HPMC growth, cell-cycle distribution was determined by flow cytometry (Fig. 2). When HPMCs were starved for 48 hours on low serum (0.5% FCS), 79.6 ± 4.1% of the cells were arrested in the G_1 phase of the cell cycle. When the cells were treated with PDGF (25 ng/mL) for 24 hours, 14.3 ± 5.2% and 26.1 ± 6.3% of the HPMCs were distributed in the S and G_2/M phases, respectively. In contrast, 81.5 ±4.5% of the HPMCs were still in the G_1 phase 24 hours after incubation with PDGF (25 ng/mL) in the presence of dipyridamole (17 μg/mL). Because dipyridamole has been shown to exert its action by increasing intracellular cAMP [12–14], we also evaluated the effect of IBMX on cell-cycle distributions of HPMCs. A similar cell-cycle distribution was observed in cells treated with PDGF (25 ng/mL) plus IBMX (1 mmol/L).

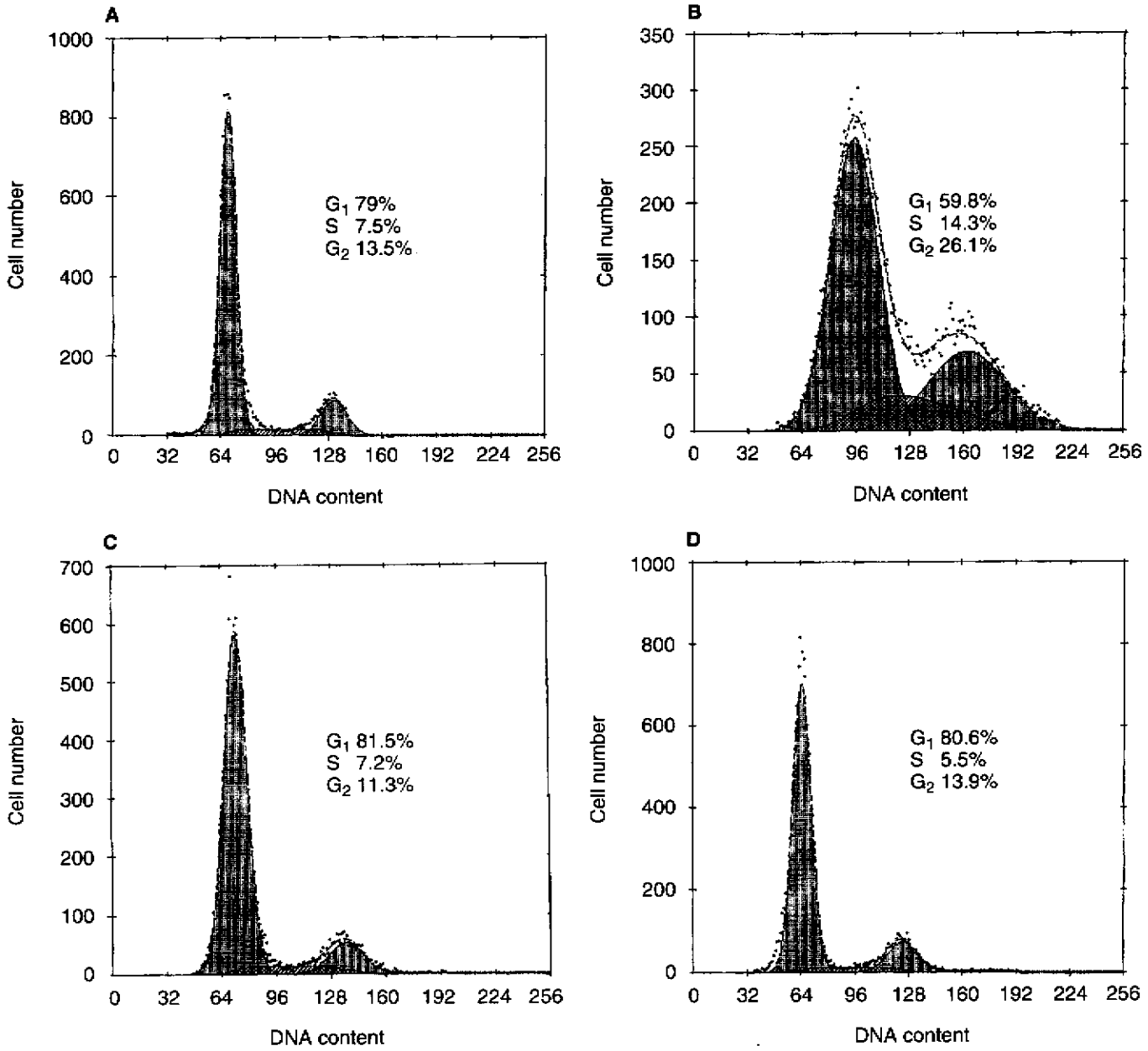

Fig. 2. Flow cytometry analysis for cell-cycle distribution. Subconfluent HPMCs were growth arrested by 0.5% FCS for 48 hours (*A*) and then changed into mediums in the presence of PDGF (25 ng/mL) alone (*B*) or (*C*) PDGF plus 17 μg/mL dipyridamole or (*D*) PDGF plus IBMX (1 mmol/L). The *x* axis shows DNA content; the *y* axis shows the number of cells. The experiments were repeated four times with similar results observed.

Dipyridamole increases intracellular cAMP levels in HPMCs

Dipyridamole is known to function as a phosphodiesterase inhibitor to increase intracellular cAMP levels [12, 13]. Thus, the effect of dipyridamole on levels of intracellular cAMP was studied. We measured cAMP levels after incubating HPMC with varying concentrations of dipyridamole (2, 6, and 17 μg/mL). In these experiments, IBMX (1 mmol/L), a known phosphodiesterase inhibitor, was used as a positive control (Fig. 3). Intracellular cAMP levels were elevated in a dose-dependent manner by dipyridamole. The addition of dipyridamole at concentrations of 6 and 17 μg/mL resulted in a significant increase of intracellular cAMP levels in HPMCs. The addition of IBMX, as expected, increased the intracellular cAMP level in HPMCs.

PKA inhibitor reversed the effect of dipyridamole

To elucidate if the growth inhibitory actions of dipyridamole was through the increased cAMP, the growth

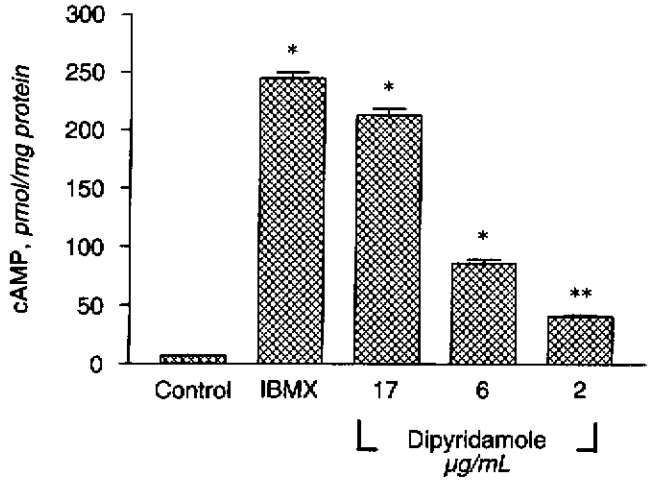

Fig. 3. Effect of dipyridamole on intracellular cAMP levels as measured by a cAMP kit. Intracellular cAMP levels were elevated in a dose-dependent manner by dipyridamole. IBMX (1 mmol/L), a known phosphodiesterase inhibitor, was used as a positive control. $*P < 0.01$, $**P < 0.05$, relative to control. All experiments were performed four times.

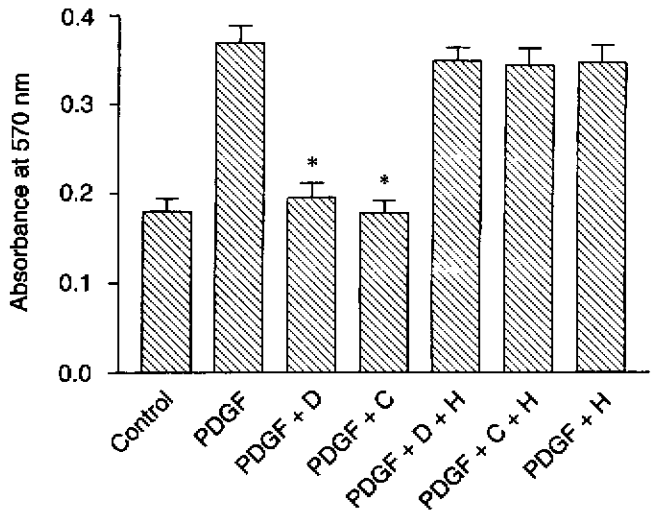

Fig. 4. Effect of dipyridamole (D, 17 μg/mL) and DBcAMP (C, 0.5 mmol/L) on PDGF-stimulated HPMC proliferation. MTT assay was performed on the fifth day. H-89 (H, 3 μmol/L) nearly completely reversed the inhibitory effect of dipyridamole or DBcAMP on PDGF-stimulated HPMC proliferation. In the absence of dipyridamole, H-89 did not independently result in HPMC proliferation. $*P < 0.01$ vs. PDGF alone. Data represent the mean ± SEM of four experiments.

inhibitory effect of DBcAMP, a membrane-permeable analogue of the cyclic nucleotide, was investigated next in cultured HPMC. The addition of DBcAMP (0.5 mmol/L) resulted in an inhibitory effect on PDGF-stimulated HPMC proliferation (Fig. 4). To confirm that the inhibitory effect of dipyridamole on HPMC proliferation was through the activated cAMP-dependent kinase (PKA) pathway, additional experiments were carried out using the cell-permeable PKA inhibitor H-89. We found that H-89 could overcome the growth inhibitory effects of dipyridamole and DBcAMP (Fig. 4). In the absence of dipyridamole or DBcAMP, H-89 did not independently result in HPMC proliferation.

Dipyridamole inhibits PDGF-induced ERK activation

The ERK cascade is the central mitogenic signaling pathway downstream of PDGF stimulation. Therefore, we studied the possible inhibitory effect of PDGF-stimulated ERK activation by dipyridamole. Western blotting of ERK1/2 phosphorylation was applied for the evaluation of ERK activities. Figure 5 shows that PDGF (25 ng/mL) increased ERK1/2 activity by 3.7-fold at 15 minutes above baseline, and maximal activation (6.2-fold) of ERK1/2 was observed at 30 minutes after addition of PDGF. Therefore, we chose this time point for additional experiments. Pretreatment of HPMC with dipyridamole (17 μg/mL) substantially reduced the ERK1/2 response to PDGF. Dipyridamole reduced PDGF-stimulated ERK1/2 activity by approximately 78.5%. Similar results were obtained following pretreatment with 0.5 mmol/L DBcAMP (data not shown). Again, the PKA inhibitor H-89 (concentration ≥3 μmol/L) completely reversed the inhibitory effect of dipyridamole or DBcAMP. In the absence of dipyridamole, H-89 did not independently activate ERK1/2 in HPMCs. Taken together, these results indicated that the inhibitory effect of dipyridamole on PDGF-stimulated HPMC proliferation, as well as downstream ERK activation, is dependent of the activation of the PKA pathway.

G_1 cyclin/CDK expression of HPMCs in the presence PDGF and dipyridamole

Because the ERK cascade is involved in gene expression of cyclin D_1 and dipyridamole arrests HPMC in the G_1/S transition and is associated with an attenuated ERK activity, we questioned whether the inhibitory effect of dipyridamole might be due to alterations of cyclin D_1 and CDK4 following PDGF stimulation. First, kinetic studies were performed to determine the protein expression of cyclin D_1. Low serum (0.5% FCS)-starved HPMCs were stimulated with 25 ng/mL PDGF and then were harvested for Western blotting analysis at the time point indicated. Western blot analysis indicated that there was a low level of protein expression for cyclin D_1 (34 kD) in quiescent (0 hour) HPMCs (Fig. 6). During PDGF stimulation, protein levels of cyclin D1 rose between 0 to 4 hours and reached maximal levels around 8 to 12 hours after stimulation. Unlike cyclin D_1, the CDK4 (32 kD) protein level remained constant in quiescent and PDGF-stimulated cells (Fig. 6). We next investigated the effects of dipyridamole and DBcAMP on protein levels of cyclin D_1 and CDK4. In contrast to our expectations, dipyridamole (Fig. 6) and DBcAMP (data not shown)

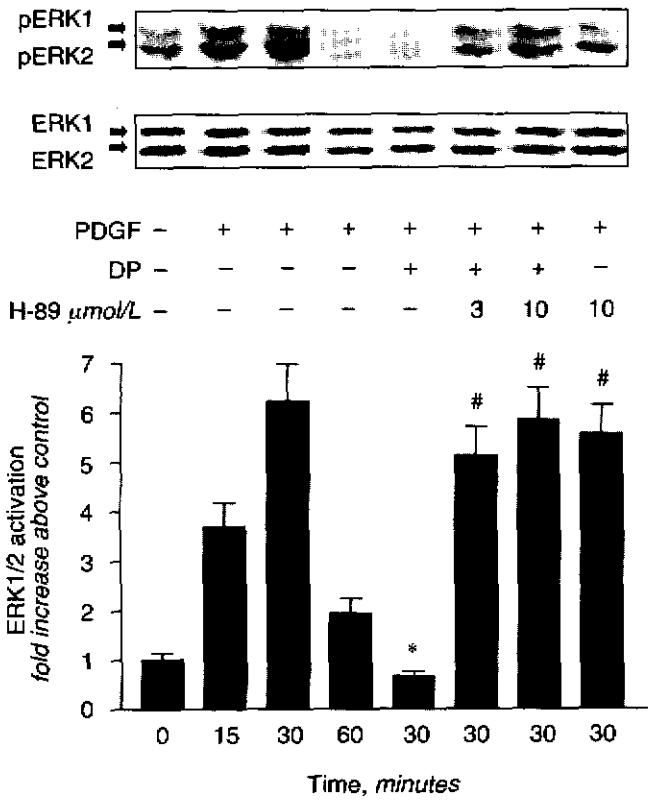

Fig. 5. Evaluation of inhibitory dipyridamole (DP, 17 μg/mL) on PDGF (25 ng/mL)-stimulated ERK1/2 activation in HPMC. Cell lysates were immunoblotted with anti-phospho-ERK1/2 for ERK activation. H-89 (unit: μmol/L) was added to overcome the inhibitory effect of dipyridamole on PDGF-stimulated ERK activation. Another aliquot of cell lysate mixtures was immunoblotted with anti-ERK1/2 antibody for protein levels, which were not significantly affected during treatment. Shown at the top is a representative blot from one experiment out of five with similar results. The mean results of densitometric analysis of four separate experiments are shown at the bottom. Values in the graph are expressed as fold increase over control. $*P < 0.01$, DP-treated vs. PDGF-treated at 30 minutes (lane 3). $\#P$ = NS vs. PDGF alone at 30 minutes (lane 3).

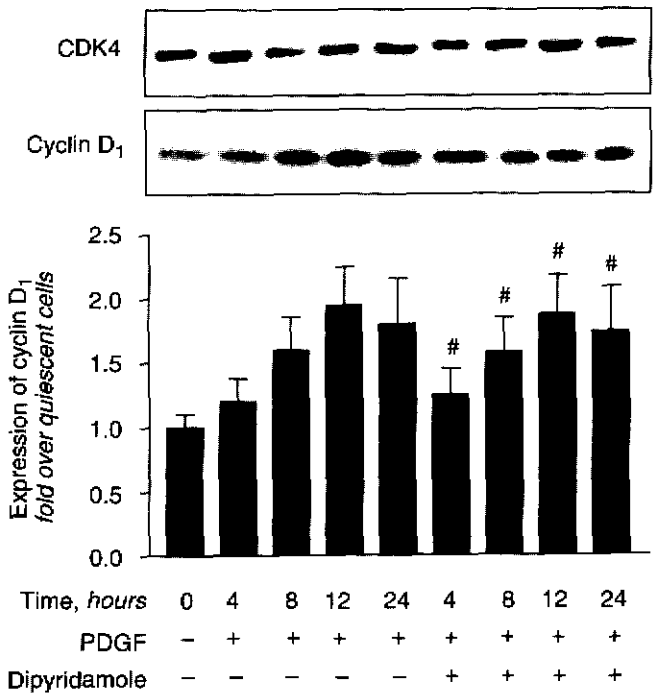

Fig. 6. Kinetics of expression of CDK4 (32 kD) and cyclin D_1 (34 kD) proteins upon stimulation with PDGF (25 ng/mL) and the effect of dipyridamole (17 μg/mL) upon their expression. Lysates (50 μg protein/lane) of HPMCs were analyzed by using specific antibodies to CDK4 and cyclin D_1. Quiescent HPMCs (0 h) were incubated with PDGF (25 ng/mL) alone or in the presence of dipyridamole (17 μg/mL) and then were harvested at indicated time points for Western blotting analysis. The blot is representative of four such studies. Densitometric analysis of four separate experiments with similar results are shown at the bottom. $\#P$ = NS vs. PDGF-treated HPMC at respective time points.

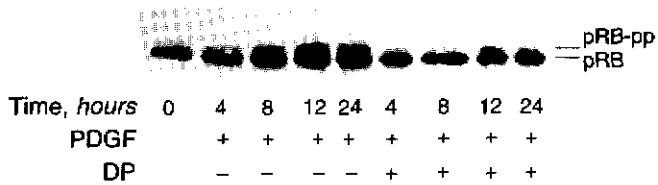

Fig. 7. Immunoblot for pRB. After PDGF treatment, hyperphosphorylation of pRB slows electrophoretic mobility of the protein, creating the appearance of a double or widened band (gel shift). Immunoblots in lysates of HPMCs showed hyperphosphorylated form of pRB as early as 8 hours after PDGF (25 ng/mL) stimulation and was observed for 24 hours. In contrast, pRB hyperphosphorylation did not occur in HPMC incubated with PDGF and dipyridamole (DP, 17 μg/mL). This experiment result was typical of 5 experiments. (control, 0.5% FCS-starved HPMCs).

had no effect on cyclin D_1 levels in PDGF-stimulated HPMC lysates. Similarly, the addition of either dipyridamole (Fig. 6) or DBcAMP (data not shown) had no effect on CDK4 protein levels.

Dipyridamole attenuates PDGF-stimulated pRB phosphorylation in HPMCs

Western blot analysis utilizing a polyclonal antibody against pRB was performed to evaluate pRB phosphorylation, which is the downstream from cyclin D_1/CDK4 complex and is necessary for G_1 phase restriction. In PDGF-stimulated HPMC, the hyperphosphorylated form of pRB, which was detected as a slower migrating band in immunoblot analysis, was readily detected within 8 hours and was observed at 24 hours (Fig. 7). In contrast, in HPMCs incubated with PDGF in the presence of dipyridamole, the hyperphosphorylated active form of pRB was almost completely blocked. Thus, the addition of dipyridamole resulted in an attenuated pRB phosphorylation.

Dipyridamole prevents PDGF-stimulated degradation of $p27^{Kip1}$ in HPMCs

In other mammalian cells, protein levels of $p27^{Kip1}$ increase in serum-deprived cells and decrease when cells

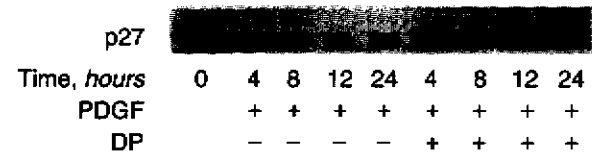

Fig. 8. Growth-arrested HPMCs were stimulated with 25 ng/mL PDGF in the presence or absence of 17 μg/mL dipyridamole (DP). At the time indicated, cellular extracts (50 μg protein/lane) were electrophoresed on 15% SDS-PAGE and immunoblotted with a polyclonal $p27^{Kip1}$ antibody. The data are representative of four such studies with similar results.

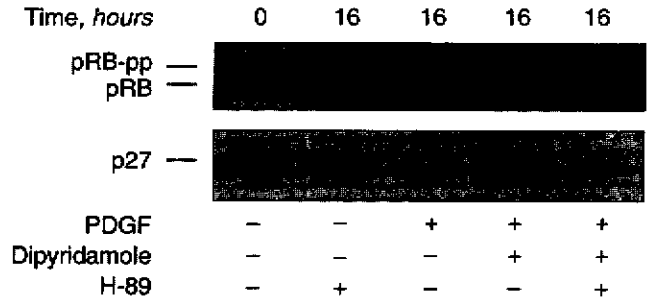

Fig. 9. Induction of p27 and hypophosphorylation of pRB by dipyridamole is PKA dependent. In experiments of H-89, HPMCs were pretreated with H-89 (10 μmol/L) for 30 minutes and then were treated with PDGF (25 ng/mL) in the presence or absence of dipyridamole (17 μg/mL) for another 16 hours. In PDGF-treated HPMCs, hyperphosphorylation of pRB and decrease in protein level of $p27^{Kip1}$ were observed. H-89, when added before dipyridamole, reverted PDGF-stimulated pRB hyperphosphorylation. The maintenance effect of $p27^{Kip1}$ by dipyridamole was also attenuated in the presence of H-89. Shown is a representative blot from one experiment out of four with similar results.

are stimulated by mitogen to enter the cell cycle [18]. In our experiments using cultured HPMCs, protein levels of $p27^{Kip1}$ decreased in a time-dependent manner after treatment with PDGF (Fig. 8). Eight hours after PDGF stimulation, $p27^{Kip1}$ protein levels decreased approximately 45% and continued to decrease, reaching a minimal level at 12 to 24 hours (nearly 15 to 20% of unstimulated cells). In contrast, dipyridamole prevented the reduction of $p27^{Kip1}$ expression by PDGF. By 24 hours, cells treated with PDGF and dipyridamole preserved nearly 80% of the $p27^{Kip1}$ expressed in unstimulated cells. With regard to the other CKIs ($p16^{INK4a}$, $p15^{INK4b}$, and $p21^{waf1/cip1}$), no significant differences of their expressions were found in dipyridamole- and/or PDGF-treated HPMCs (data not shown).

Stabilization of $p27^{Kip1}$ and hypophosphorylation of pRB by dipyridamole is PKA-dependent

Since dipyridamole elevates intracellular cAMP levels, we assumed that the regulatory effect of dipyridamole on $p27^{Kip1}$ and pRB could be through the PKA pathway. To examine the validity of this hypothesis, H-89 was used to assess the role of PKA in $p27^{Kip1}$ induction and in pRB hypophosphorylation by dipyridamole in PDGF-treated HPMCs. As shown in Figure 9, PDGF induced a dramatic decrease in $p27^{Kip1}$ levels. In H-89 pre-treated HPMC, dipyridamole was unable to prevent $p27^{Kip1}$ elimination by PDGF. Further, PDGF was able to induce pRB hyperphosphorylation in HPMC when H-89 was added before dipyridamole. Taken together, these results suggest that the cell-cycle regulatory effect of dipyridamole in HPMC is PKA-dependent.

DISCUSSION

Normal turnover of the mesothelium is essential to maintain peritoneal membrane integrity. However, the overproliferation of HPMCs and subsequent accumulation of extracellular matrix may contribute to the development of PF. Our study demonstrates an inhibitory effect of dipyridamole on PDGF-stimulated HPMC proliferation. The usual plasma level of dipyridamole after an oral administration of a conventional dosage (150 to 400 mg per day) is about 1 to 3 μg/mL [25]. In our culture system, an inhibitory effect of dipyridamole was demonstrated starting at a concentration of 6 μg/mL (Fig. 1). However, the serum level may not represent exactly the tissue level of dipyridamole. Dipyridamole can be administered through an intraperitoneal route in patients on peritoneal dialysis, and, therefore, a higher intraperitoneal concentration of dipydiamole may be achieved. This implies that dipyridamole has therapeutic value for the prevention or alleviation of PF in vivo as well as in daily practice.

One of the cellular mechanisms of dipyridamole is through attenuation of the ERK cascade of HPMC. To our knowledge, this is the first study to elucidate the role and activation of the ERK cascade in HPMCs. Himmelfarb and Couper demonstrated that dipyridamole, by antagonizing the ERK1/2, inhibited PDGF-induced vascular SMC proliferation [8]. In accordance with those findings, in HPMC we observed a reduced ERK1/2 response to PDGF by dipyridamole (Fig. 5). Dipyridamole has been well documented to exert its pharmacological effects via increasing intracellular cAMP [12–14]. A few studies have reported that cAMP inhibits PDGF-induced mitogenesis through attenuating ERK activity [26, 27]. To examine whether the suppressive effect of dipyridamole on ERK1/2 activity in HPMC was also through increased cAMP, we examined the effects of raising intracellular cAMP on ERK1/2 activity in HPMCs. Figure 5 shows that dipyridamole (17 μg/mL) suppressed PDGF-stimulated ERK1/2 activation in HPMC. Moreover, we further demonstrated that the inhibitory effect of dipyridamole could be reversed in the presence of H-89. Taken together, these results indicate that the cAMP-PKA pathway most likely mediates the suppression of PDGF-stimulated ERK1/2 activation by dipyridamole.

Another mechanism for the inhibitory effect of dipyridamole is through alterations of the cell-cycle progression in HPMC. Using flow cytometry (Fig. 2), we demonstrated, for the first time to our knowledge, that dipyridamole inhibits HPMC at the G_1 phase. In other cell types [28, 29], it had been postulated that cAMP prevents G_1 phase cell-cycle progression by suppressing the expression of cyclin D_1 and CDK4. As dipyridamole inhibits HPMCs via the cAMP-PKA pathway, this G_1 arrest of HPMCs was assumed to result from an impaired expression of cyclin D_1 and/or CDK4 by increased intracellular cAMP. However, in our experiments of HPMCs, dipyridamole showed no effect on levels of cyclin D_1 and CDK4 (Fig. 6). Similar effects on cyclin D_1 and CDK4 were observed after addition of DBcAMP (data not shown). Kato et al demonstrated in a macrophage cell line that cAMP had no effect on cyclin D_1 levels [30]. The previously mentioned findings highlight the fact that while antiproliferative agents target cell cycle machinery, the exact mechanisms differ depending on the agent and the cell types. As dipyridamole has no effect on the cyclin D_1 and CDK4 of HPMC (Fig. 6), the blockade of pRB phosphorylation observed in dipyridamole-treated HPMC (Fig. 7) may be based on other mechanisms.

The other potential mechanism for this blockade of pRB phosphorylation may be through antagonizing the cyclin D_1/CDK4 activity by $p27^{Kip1}$ [31]. It has been postulated that the suppression of $p27^{Kip1}$ results in cell-cycle exit from quiescence [32]. The relative levels of $p27^{Kip1}$ versus those of cyclin D_1/CDK4 are crucial in determining whether pRB is activated (phosphorylated) [17, 18]. A role for cAMP in maintenance of $p27^{Kip1}$ by inhibiting its depletion has been suggested [31]. Our data support this notion. In this work, dipyridamole prevented a marked decline of $p27^{Kip1}$ in response to PDGF (Fig. 8). Stabilization of $p27^{Kip1}$ and hypophosphorylation of pRB by dipyridamole is PKA-dependent (Fig. 9). Our data suggest that in PDGF-treated HPMC, although the protein levels of cyclin D_1 and CDK4 were not changed by dipyridamole, the preservation of $p27^{Kip1}$ by dipyridamole may contribute to its effect of cell-cycle arrest. We currently are investigating the mechanisms by which dipyridamole prevents the reduction of $p27^{Kip1}$ in PDGF-treated HPMC. They may occur via the ubiquitin-proteasome pathway [33] and/or inhibition of the activation of ERK by cAMP [34]. Future studies should address which mechanism is predominantly operative in HPMCs.

In summary, dipyridamole attenuates ERK cascades of HPMC and modulates cell-cycle progression in response to PDGF. There are three important findings in this study. First, in HPMC, the ERK cascade acts as a critical step in downstream signaling of PDGF stimulation. Second, dipyridamole suppresses PDGF-stimulated ERK1/2 activation through the cAMP-PKA pathway. Finally, dipyridamole arrests HPMC in the G_1/S transition by preventing the depletion of $p27^{Kip1}$ and modulating pRB phosphorylation. Dipyridamole may have therapeutic value for future clinical application in PF prevention.

ACKNOWLEDGMENTS

This study was supported by grants from the National Science Council (NSC 89-2314-B-002-507), Ta-Tung Kidney Foundation, and Mrs. Hsiu-Chin Lee Kidney Research Fund, Taipei. The authors thank Ms. Shu-Ying Chou and Mr. Chin-Ching Yang for their technical assistance.

Reprint requests to Tun-Jun Tsai, M.D., Department of Internal Medicine, National Taiwan University Hospital, Number 7, Chung-Shan South Road, Taipei, Taiwan, R.O.C.
E-mail: paul@ha.mc.ntu.edu.tw

APPENDIX

Abbreviations used in this article are: cAMP, cyclic adenosine 3′5′-monophosphate; CAPD, continuous ambulatory peritoneal dialysis; CDK, cyclin-dependent kinase; CKI, cyclin kinase inhibitors; DBcAMP, dibutyryl-cAMP; DP, dipyridamole; EIA, enzyme immunoassay; ERK, extracellular signal-regulated protein kinase; FCS, fetal calf serum; HPMC, human peritoneal mesothelial cells; IBMX, 3-isobutyl-1-methylxanthine; LDH, lactate dehydrogenase; MTT, 3-[4,5-dimethylthiazol-2-yl]-2,5-diphenyltetrazolium bromide; PBS, phosphate-buffered saline; PD, peritoneal dialysis; PDGF, platelet-derived growth factor; PF, peritoneal fibrosis; PKA, protein kinase A; PMSF, phenylmethylsulfonyl fluoride; pRB, retinoblastoma gene product; PVDF, polyvinylidene difluoride; SMC, smooth muscle cells.

REFERENCES

1. Dobbie JW, Anderson JD, Hind C: Long-term effects of peritoneal dialysis on peritoneal morphology. *Perit Dial Int* 14(Suppl 3):S16–S20, 1994
2. Gotloib L, Waisbrut V, Shostak A, Kushnier R: Acute and long-term changes observed in imprints of mouse mesothelium exposed to glucose-enriched, lactated, buffered dialysis solutions. *Nephron* 70:466–477, 1995
3. Beavis MJ, Williams JD, Hoppe J, Topley N: Human peritoneal fibroblast proliferation in 3-dimensional culture: Modulation by cytokines, growth factors and peritoneal dialysis effluent. *Kidney Int* 51:205–215, 1997
4. Owens MW, Milligan SA: Growth factor modulation of rat pleural mesothelial cell mitogenesis and collagen synthesis: Effects of epidermal growth factor and platelet-derived factor. *Inflammation* 18:77–87, 1994
5. Force T, Bonventre JV: Growth factors and mitogen-activated protein kinases. *Hypertension* 31(1 Pt 2):152–161, 1998
6. Yang Z, Oemar BS, Carrel T, *et al*: Different proliferative properties of smooth muscle cells of human arterial and venous bypass vessels: Role of PDGF receptors, mitogen-activated protein kinase, and cyclin-dependent kinase inhibitors. *Circulation* 97:181–187, 1998
7. Bornfekdt KE, Campbell JS, Koyama H, *et al*: The mitogen-activated protein kinase pathway can mediate growth inhibition and proliferation in smooth muscle cells: Dependence on the availability of downstream targets. *J Clin Invest* 100:875–885, 1997
8. Himmelfarb J, Couper L: Dipyridamole inhibits PDGF- and bFGF-induced vascular smooth muscle cell proliferation. *Kidney Int* 52:1671–1677, 1997
9. Plevin R, Malarkey K, Aidulis D, *et al*: Cyclic AMP inhibits PDGF-stimulated mitogen-activated protein kinase activity in rat aortic smooth muscle cells via inactivation of c-Raf-1 kinase and induction of MAP kinase phosphatase-1. *Cell Signal* 9:323–328, 1997
10. Robinson CJ, Scott PH, Allan AB, *et al*: Treatment of vascular smooth muscle cells with antisense phosphorothioate oligodeoxynucleotides directed against p42 and p44 mitogen-activated protein

kinases abolishes DNA synthesis in response to platelet-derived growth factor. *Biochem J* 320(Pt 1):123–127, 1996
11. SALE EM, ATKINSON PG, SALE GJ: Requirement of MAP kinase for differentiation of fibroblasts to adipocytes, for insulin activation of p90 S6 kinase and for insulin or serum stimulation of DNA synthesis. *EMBO J* 14:674–684, 1995
12. FITZGERALD GA: Dipyridamole. *N Engl J Med* 316:1247–1257, 1987
13. HILLIS GS, DUTHIE LA, MACLEOD AM: Dipyridamole inhibits human mesangial cell proliferation. *Nephron* 78:172–178, 1998
14. TSAI TJ, LIN RH, CHANG CC, *et al*: Vasodilator agents modulate rat glomerular mesangial cell growth and collagen synthesis. *Nephron* 70:91–100, 1995
15. HANEDA M, ARAKI SI, SUGIMOTO T, *et al*: Differential inhibition of mesangial MAP kinase cascade by cyclic nucleotides. *Kidney Int* 50:384–391, 1996
16. SHERR CJ: Mammalian G1 cyclins. *Cell* 73:1059–1065, 1993
17. WEINBERG RA: The retinoblastoma protein and the cell cycle. *Cell* 81:323–330, 1995
18. SHERR CJ, ROBERTS JM: Inhibitors of mammalian G1 cyclin-dependent kinases. *Genes Dev* 9:1149–1163, 1995
19. COATS S, FLANAGAN WM, NOURSE J, ROBERTS JM: Requirement of $p27^{Kipl}$ for restriction point control of the fibroblast cell cycle. *Science* 272:877–880, 1996
20. SHANKLAND SJ, PIPPIN J, FLANAGAN M, *et al*: Mesangial cell proliferation mediated by PDGF and bFGF is determined by levels of the cyclin kinase inhibitor $p27^{Kipl}$. *Kidney Int* 51:1088–1099, 1997
21. FANG CC, YEN CJ, CHEN YM, *et al*: Pentoxifylline inhibits human peritoneal mesothelial cell growth and collagen synthesis: Effects on TGF-β. *Kidney Int* 57:2626–2633, 2000
22. FANG CC, YEN CJ, CHEN YM, *et al*: Hydralazine inhibits human peritoneal mesothelial cell proliferation and collagen synthesis. *Nephrol Dial Transplant* 11:2276–2281, 1996
23. SMITH PK, KROHN RI, HERMANSON GT, *et al*: Measurement of protein using bicinchoninic acid. *Anal Biochem* 150:76–85, 1985
24. MATSUSHIME H, ROUSSEL MF, ASHMUN RA, SHERR CJ: Colony-stimulating factor 1 regulates novel cyclins during the G1 phase of the cell cycle. *Cell* 65:701–713, 1991
25. SEGALL GM, DAVIS MJ: Variability of serum drug level following a single oral dose of dipyridamole. *J Nucl Med* 29:1662–1669, 1988
26. COOK SJ, MCCORMICK F: Inhibition by cAMP Ras-dependent activation of Raf. *Science* 262:1069–1072, 1993
27. HORDIJK PL, VERLAAN I, JALINK K, *et al*: cAMP abrogates the p21ras-mitogen-acitvated protein kinase pathway in fibroblasts. *J Biol Chem* 269:3534–3538, 1994
28. VADIVELOO PK, VAIRO G, NOVAK U, *et al*: Differential regulation of cell cycle machinery by various antiproliferative agents is linked to macrophage arrest at distinct checkpoints. *Oncogene* 13:599–608, 1996
29. WILLIAMSON EA, BURGESS GS, EDER P, *et al*: Cyclic AMP negatively controls c-myc transcription and G1 cell cycle progression in p210 BCR-ABL transformed cells: Inhibitory activity exerted through cyclin D1 and cdk4. *Leukemia* 11:73–85, 1997
30. KATO JY, MATSUOKA M, STROM DK, SHERR CJ: Regulation of cyclin D-dependent kinase 4 (cdk4) by cdk4-activating kinase. *Mol Cell Biol* 14:2713–2721, 1994
31. KATO JY, MATSUOKA M, POLYAK K, *et al*: Cyclic AMP-induced G1 phase arrest mediated by an inhibitor ($p27^{Kip1}$) of cyclin-dependent kinase 4 activation. *Cell* 79:487–496, 1994
32. LADHA MH, LEE KY, UPTON TM, *et al*: Regulation of exit from quiescence by p27 and cyclin D1–CDK4. *Mol Cell Biol* 18:6605–6615, 1998
33. ALESSANDRINI A, CHIAUR DS, PAGANO M: Regulation of the cyclin-dependent kinase inhibitor p27 by degradation and phosphorylation. *Leukemia* 11:342–345, 1997
34. KAWADA M, YAMAGOE S, MURAKAMI Y, *et al*: Induction of p27kip1 degradation and anchorage independence by Ras through the MAP kinase signaling pathway. *Oncogene* 15:629–637, 1997

Kidney International, Vol. 59 (2001), pp. 2316–2324

Dipyridamole inhibits human peritoneal mesothelial cell proliferation in vitro and attenuates rat peritoneal fibrosis in vivo

KUAN-YU HUNG, REN-SHI SHYU, CHENG-CHUNG FANG, CHIEN-CHEN TSAI, PO-HUANG LEE, TUN-JUN TSAI, and BOR-SHEN HSIEH

Departments of Internal Medicine, Emergency Medicine, Surgery, and Pathology, National Taiwan University Hospital, Taipei, Taiwan, Republic of China

Dipyridamole inhibits human peritoneal mesothelial cell proliferation in vitro and attenuates rat peritoneal fibrosis in vivo.

Background. Peritoneal fibrosis (PF) is one of the most serious complications after long-term continuous ambulatory peritoneal dialysis (CAPD). Proliferation of human peritoneal mesothelial cells (HPMC) and matrix over-production are regarded as the main processes predisposing to PF. Dipyridamole (DP) has been reported to have potential as an antiproliferative and antifibrotic agent. We thus investigated the effect of DP in inhibiting proliferation and collagen synthesis of HPMC. A rat model of peritonitis-induced PF was also established to demonstrate the in vivo preventive effect of DP.

Methods. HPMC was cultured from human omentum by an enzyme digestion method. Cell proliferation was measured by the methyltetrazolium assay. Intracellular cAMP was measured using an enzyme immunoassay (EIA) kit. Total collagen synthesis was measured by ^{3}H-proline incorporation assay. Expression of collagen α1 (I) and collagen α1 (III) mRNAs was determined by Northern blotting. The rat model of peritonitis-induced PF was developed by adding dextran microbeads (Cytodex, 8 mg/1 mL volume) to a standardized suspension (3×10^9) of *Staphylococcus aureus*. DP was administrated via intravenous infusion (4 mg in 1 h) daily for seven days. Macroscopic grading of intraperitoneal adhesions and histological analyses of peritoneal thickness and collagen expression were performed.

Results. Addition of DP to HPMC cultures suppressed serum-stimulated cell proliferation and collagen synthesis. The antimitogenic and antifibrotic effects of DP appear to be predominantly mediated through the cAMP pathway, as DP increased intracellular cAMP in a dose-dependent manner. The macroscopic grade of intraperitoneal adhesion and peritoneal thickness were both significantly increased in animals treated with Cytodex plus *S. aureus*; on the other hand, DP attenuated these fibrotic changes with statistical significance ($P < 0.01$). Analysis of gene expression of collagen α1 (I) and α1 (III) in the peritoneal tissue of experimental animals yielded similar results.

Conclusions. This study suggests that dipyridamole may have therapeutic potential in treating peritoneal fibrosis.

Key words: mesothelial cell, collagen, animal model, CAPD, mitogenesis, cAMP, uremia, extracellular matrix.

Received for publication August 31, 2000
and in revised form December 26, 2000
Accepted for publication January 10, 2001

Continuous ambulatory peritoneal dialysis (CAPD) has gained increasing popularity in the treatment of uremia, and peritoneal fibrosis (PF) is one of the most serious complications after long-term CAPD [1]. It had been postulated that proliferation of human peritoneal mesothelial cells (HPMC) accompanied by matrix expansion plays a fundamental role in the pathogenic process of PF [2]. Pharmacological interventions that can inhibit the proliferation of HPMC and/or matrix formation thus may be beneficial for the prevention or retardation of the progression of PF.

Dipyridamole (DP; 2,6-bis[diethanolamino]-4,8-dipiperidinopyrimido-[5,4-d]-yrimidine) is an antiplatelet agent with an undefined mechanism of action [3]. In addition to its antiplatelet activity, DP has been shown to exert antiproliferative effects on rat vascular smooth muscle cells [4] and human mesangial cells [5]. We have previously shown that DP exerts an antifibrogenic effect on rat mesangial cells by inhibiting cell proliferation and reduce cell expression of type I collagen mRNA [6]. However, the inhibitory effect of DP on HPMC proliferation has never been reported. Accordingly, the first aim of the present study was to investigate in vitro the inhibitory effect of DP on HPMC proliferation and collagen accumulation.

The importance of bacterial peritonitis as a leading etiological agent of PF in long-term CAPD patients is well established [7]. Several studies have demonstrated that *Staphylococcus aureus* is one of the most common organisms causing CAPD peritonitis. An experimental infection model of *S. aureus* peritonitis was attempted

by Calame et al [8]; however, their infection model was less severe than ours and no study has focused specifically on the pathogenesis of PF. Another rat model of PF induced by *Escherichia coli* has also been postulated [9]. Nevertheless, such infection is rare in the CAPD population and the induction of PF was not successful. Therefore, we sought to establish a model that more closely mimicked peritonitis-related PF in CAPD patients. The second aim of our work was to establish a rat model of PF developed secondary to *S. aureus* peritonitis. The third aim was to demonstrate the in vivo preventive effect of DP on this experimental PF rat model.

METHODS

Materials

Fetal calf serum (FCS) was obtained from Biochrome KG (Berlin, Germany). Culture flasks and plates were purchased from Corning (Corning, NY, USA) and precoated with 1.6 μg/cm² of Vitrogen 100® (Celtrix Lab, Palo Alto, CA, USA) before cell loading. Trypsin-ethylenediaminetetraacetic acid (EDTA), RPMI-1640 medium, glutamine, and trypan blue were obtained from Gibco (Grand Island, NY, USA). Bovine serum albumin (BSA), 3-[4,5-dimethylthiazol-2-yl]-2,5-diphenyltetrazolium bromide (MTT), 3-isobutyl-1-methylxanthine (IBMX) and other tissue culture reagents were purchased from Sigma (St. Louis, MO, USA). ^{3}H-proline was purchased from DuPont NEN (Boston, MA, USA). The enzyme immunoassay (EIA) kits for cyclic adenosine monophosphate (cAMP) were obtained from Cayman Chemical (Ann Arbor, MI, USA). Human collagen α1 (I) and collagen α1 (III) cDNAs were purchased from American Type Culture Collection (Rockville, MD, USA). Agents used to isolate the total RNA and Northern blot analysis were obtained from Boehringer Mannheim (Mannheim, Germany) unless otherwise specified. DP was generously provided by Boehringer Ingelheim (Ingelheim, Germany). All other chemicals used were of analytical grade.

Human peritoneal mesothelial cell culture

Specimens of human omentum were obtained from abdominal surgical procedures for elective gastric cancer resection and the omentum was essentially normal. The HPMC culture was carried out as we previously reported [10, 11]. Briefly, the surgically removed human omentum was washed three times with PBS and then digested with trypsin EDTA (0.125%) for 15 minutes. After centrifugation, the cell pellet was washed with culture medium and then seeded into a vitrogen-coated (1 mg/mL) flask. The medium was changed on the third day. RPMI-1640 medium containing 20% FCS, penicillin (100 U/mL), streptomycin (100 μg/mL), and insulin (30 μg/mL) was used. After two to four days, the cells became confluent and were subcultured with medium containing 10% FCS. HPMC were identified by the presence of vimentin and cytokeratin without desmin or factor VIII-related antigen using the immunofluorescence method. All experiments were performed in cells from passages 1 to 3.

Cell proliferation assay

A modified MTT assay was used to evaluate PMC proliferation as previously reported [10]. The amount of MTT uptake (absorbance at 570 nm) by HPMC was found to vary linearly with cell numbers ranging from 4000 cells/well to 12.8×10^4 cells/well in 96-well plates [10]. We loaded 5000 cells/well for each MTT assay. Cells growing in the log phase were trypsinized and plated down in 96-well plates with RPMI-1640 medium containing 10% FCS. Various concentrations of treating agents were added after overnight plating. The medium and drug were changed every three days. After additional incubations of 24 to 120 hours, 20 μL MTT solution (5 mg/mL in PBS) was added to the culture medium. Cells were incubated further at 37°C for four hours, after which the medium was replaced by 100 μL ethanol. Absorbance at the reference wavelength of 630 nm and test wavelength of 570 nm was measured by an enzyme-linked immunosorbent assay (ELISA) reader. All samples were tested in pentaplicate. The inhibition of HPMC growth was calculated as follows [10]:

$$\text{Percentage of inhibition} = 1 - \frac{\text{Absorbance of (test well} - \text{initial plating)}}{\text{Absorbance of (control} - \text{initial plating)}} \times 100\%$$

Intracellular cyclic-AMP assay

We loaded 3×10^5 HPMC cells/well into a six-well plate with RPMI-1640 medium containing 10% FCS. After cells became subconfluent, they were washed twice with warm RPMI-1640 medium and then mixed with various concentrations of agents. After five minutes of incubation, the supernatants were discarded and ice-cold 95% methanol was added to each well. After 30 minutes of incubation at 4°C, the supernatants evaporated and cAMP was measured using EIA kits. The cells in wells were lysed by 0.1 N NaOH and protein content was measured by bicinchoninic acid assay, using BSA as a standard [12]. All experiments were performed four times.

Assay of total collagen synthesis

A ^{3}H-proline incorporation assay was used to measure total collagen production, as we previously described [11]. Briefly, HPMC were seeded in 96-well plates at a density of 2.5×10^4 cells/well in 200 μL RPMI-medium supplemented with 10% FCS. After 48 hours, cells became confluent. Then the medium was replaced with ascorbic acid (50 μg/mL) in the presence of various concentrations of DP. After incubation for another 48 hours,

cells were labeled with 0.5 μCi of ^{3}H-proline (100 Ci/mmol) and 50 μg/mL β-aminopropionitrile during the final 24 hours of incubation. ^{3}H-proline incorporation into pepsin-resistant, salt-precipitated collagen was measured with a liquid scintillation counter. The cell numbers were determined simultaneously by MTT assay in identically treated microplates. The results were expressed as disintegrations per minute (dpm) of ^{3}H-proline per 10^4 cells and were compared to the control values. All experiments were performed in triplicate.

Northern blot analysis

To determine the effect of DP on collagen gene expression, HPMC were grown in RPMI supplemented with 10% FCS until subconfluency. HPMC were then treated with fresh medium in the absence or presence of various concentrations of DP. At indicated time intervals, cells were harvested for isolation of total RNA, as previously described [11]. The concentration of each sample was determined using spectrophotometry with the absorbance at 260 nm (A_{260}). The purity of each sample was determined based on the ratio of A_{260} to A_{280}. Ten micrograms of RNA were electrophoresed on a 1% agarose gel containing 1 mol/L formaldehyde in MOPS buffer (0.2 mol/L morpholinopropanesulfonic acid, 0.05 mol/L Na acetate, 0.01 mol/L EDTA). Equivalency of sample loading and lack of degradation were verified by ethidium bromide staining of the 28 S and 18 S rRNA bands. The RNA then was transferred to nylon membranes by overnight capillary action and followed by fixation in a UV cross-linker.

Because HPMCs mainly express type I and III collagens [13], both of these were used as probes for Northern blotting. A 1.5-kb EcoRI fragment of collagen α1 (I) and a 0.7-kb *Hin*dIII/EcoRI fragment of collagen α1 (III) were subcloned, respectively, into pBSII/SK (Stratagene, La Jolla, CA, USA) and used as templates for in vitro transcription of antisense digoxigenin-conjugated riboprobes (Boehringer Mannheim) according to the manufacturer's instructions. The blots were developed using CSPD (Boehringer Mannheim) as the substrate for alkaline phosphatase, as described by the supplier. The signal intensity recorded on x-ray film was then quantified with computerized densitometry and normalized against the signal of glyceraldehyde-3-phosphate dehydrogenase (GAPDH) messages.

Animal model

Animals. Male Wistar rats (weighing 180 to 200 g; Simonson Lab., Gilroy, CA, USA) were maintained on a 12-hour light/dark cycle and provided with food and water ad libitum. All work was carried out in accordance with American Association for Accreditation for Laboratory Animal Care (AAALAC) regulations.

Preparation and induction of peritonitis. The *S. aureus* strain ATCC 25923 (American Type and Culture Collection, MD, USA) was used throughout the study. Before each experiment, a fresh six to nine hour culture in a brain-heart infusion broth (BHI, Oxoid, Basingstoke, UK) was made in an agitated water bath at 37°C. Serial dilutions were prepared and plated to determine the actual inoculum sizes used. To enhance local bacterial infection in the rat peritoneal cavity, dextran beads (Cytodex; Sigma Chemicals, St. Louis, MO, USA) were added to the bacterial suspension for inoculation as described by Ford et al [14]. Beads were first prepared as a stock solution by suspending 1 g in 50 mL of PBS, and were autoclaved before use. Aliquots of the Cytodex suspension were added to the broth with or without bacteria (3×10^9 CFU), and then additional broth was added for a final volume of 1 mL for the inoculation. Rats were divided into groups, tagged, and given an intraperitoneal (IP) injection of the prepared suspension with a 1 mL tuberculin syringe.

Pilot study to establish the experimental protocol. In a pilot experiment, 30 rats were used to establish the experimental model of peritonitis and induction of PF. To examine the toxicity of Cytodex, six rats that had received IP injections of various volumes and concentrations of Cytodex suspension were observed for 72 hours. Another six rats received continuous intravenous infusion (IVF) of DP (4 mg in 1 hour) via a jugular vein catheter, which did not produce side effects. During the observation period, all rats were active and no deaths were recorded. After being anesthetized with ketamine [75 mg/kg body weight intramuscularly (IM)], 18 rats received IP injections of various combinations of bacteria and Cytodex suspension solution. After this procedure, these animals were randomly allocated into two experimental groups, and were either left without further treatment or treated daily with IVF of DP through implanted jugular vein catheters. Through these pilot experiments, we expected to successfully induce a peritonitis-related PF. The induced peritonitis in rats was to be serious enough to cause the subsequent development of PF but not death. Based on the results of the pilot experiments, the experimental design for the in vivo animal study was adapted as described in the next section.

Experimental design. In each experiment, rats were divided into four groups of 10 rats per group. Group 1 received IP injections of bacteria (3×10^9 CFU) only, group 2 received Cytodex (8 mg/1 mL volume) only, group 3 received bacteria mixed with Cytodex (3×10^9 CFU bacteria plus 8 mg Cytodex in a total volume of 1 mL), and group 4 received the same manipulation as group 3 except with an additional daily IVF of DP (4 mg in 60 min) for seven days. The experiment was completed on day eight. Ten additional healthy rats that received IP injections of 1 mL 0.9% saline were used as the control group.

Morphological and histochemical analysis of the peritoneal cavity

Gross adhesion scoring system. After anesthesia, the rat abdomen was completely opened for an objective observer to assess the adhesions. For this purpose, a scale developed by Mullarniemi et al was applied with modifications [15]. A score of 0 indicated no adhesion, 1 indicated one to three separate adhesions, 2 indicated three or more distinctly separate adhesions, and 3 indicated diffuse, sheet-like adhesions. Based on the results of pilot experiments described earlier, we found that adhesions may develop between the liver and omentum, the omentum and intestinal wall, the intestine and abdominal wall, or between the intestine and stomach. Therefore, these fields were checked separately, making 12 the highest possible score. The total scores of each rat were recorded for statistical analysis.

Histological analysis. At the time of sacrifice, peritoneal tissue specimens were taken from the gut with the mesentery and from the liver for histological analysis. After being formalin fixed and paraffin embedded, tissue was cut into 5 μm thick sections and processed using a standard hematoxylin and eosin stain and Masson's Trichrome stain. The thickness of the connective tissue between the mesothelium and the liver surface or intestine wall was objectively evaluated, as previously reported [16, 17]. Each tissue section was measured at five random locations. Six tissue sections per rat (3 from the gut, 3 from the liver surface) were examined. The average thickness (μm) of each tissue section was recorded for statistical analysis between different groups.

Northern blot analysis of collagen content. Animals were sacrificed, and tissue samples of the omentum, adhesion strands, and the right upper quadrant of the abdominal wall were taken and then immediately frozen in an ethanol/dry ice bath and stored at −70°C. Total RNA was extracted from homogenized tissue using TRIzol reagent (Life Technology, Grand Island, NY, USA) according to the manufacturer's protocol. Total RNA (20 μg/lane) was electrophoresed on a 1% agarose/1 mol/L formaldehyde gel and then transferred to a nylon membrane. Hybridization, washing, and autoradiography were performed as described previously for Northern blot analysis in cultured HPMC.

Statistical analysis

Results are expressed as mean ± SD, unless stated otherwise. Statistical analyses were carried out using SPSS/Windows (SPSS Inc.) and StatView 4.1 (Abacus Concept Inc., Berkeley, CA, USA) software on a personal computer. Statistical significance ($P < 0.05$) was evaluated by the Student t test or one-way ANOVA and modified t test with application of the Bonferroni correction.

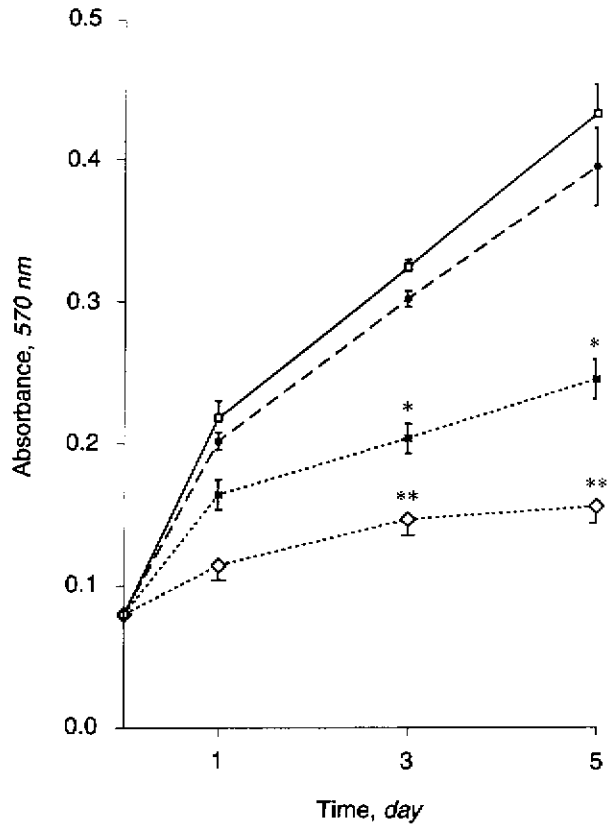

Fig. 1. Dipyridamole (DP) inhibits human peritoneal mesangial cell (HPMC) growth. Time-response curve: Varying concentrations of DP were added after overnight plating of HPMC and further incubated with 10% fetal calf serum (FCS) for one to five days. The experiment was repeated four times. Symbols are: (□) 10% FCS; (●) 10% FCS + 2 μg/mL DP; (■) 10% FCS + 6 μg/mL DP; (◇) 10% FCS + 17 μg/mL DP; $*P < 0.05$ and $**P < 0.01$, compared to 10% FCS.

RESULTS

In vitro studies

Dipyridamole inhibited serum-stimulated proliferation of HPMC. Growth curve experiments were performed to evaluate the effect of DP on serum-stimulated HPMC proliferation. In time response experiments (Fig. 1), DP at concentrations above 6 μg/mL caused a dose-dependent inhibition of HPMC. The dose-response study of the effect of increasing concentrations of DP on HPMC proliferation is shown in Figure 2. When compared to the control group (10% FCS), growth inhibition was statistically significant ($P < 0.05$) starting at 6 μg/mL of DP. The percentages of inhibition by DP at concentrations of 6 and 17 μg/mL were 44% and 53%, respectively. We therefore used a higher concentration (17 μg/mL) of DP in the following experiments to study its antifibrotic effect on HPMC. To exclude the possibly toxic effect of such a concentration of DP on proliferative HPMC, a cell viability test was performed using the trypan blue exclusion method and by measuring the lactate dehy-

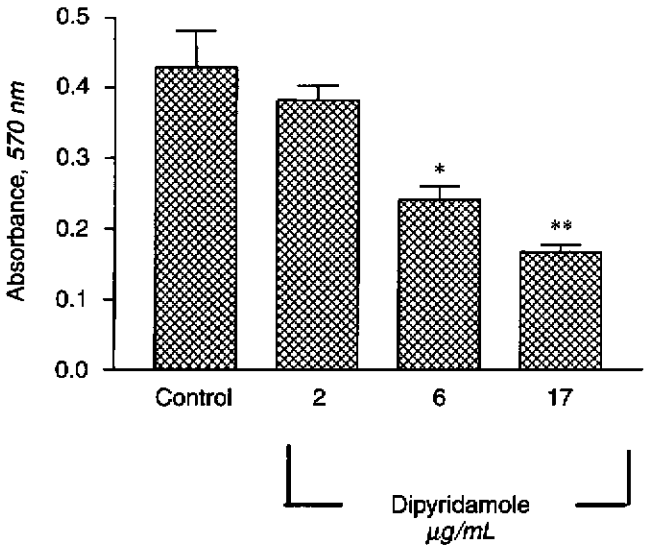

Fig. 2. Effect of DP on serum-stimulated HPMC proliferation. For the dose-response study, HPMC were incubated for 120 hours after addition of varying concentrations of DP. Data represent the mean ± SD from three independent experiments performed in triplicate. $*P <$ 0.05 and $**P < 0.01$, compared to control.

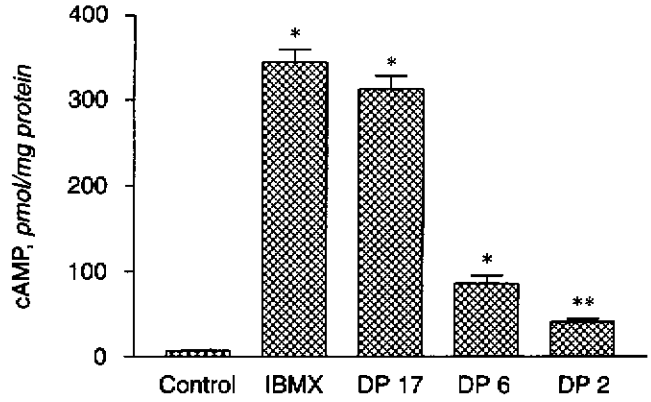

Fig. 3. Effect of DP (μg/mL) on intracellular cAMP levels (pmol/mg protein) as measured by a cAMP kit. Intracellular cAMP levels were elevated in a dose-dependent manner by DP. IBMX is 3-isobutyl-1-methylxanthine. Data represent the mean ± SD from three independent experiments performed in triplicate. $*P < 0.01$ and $**P < 0.05$, relative to control.

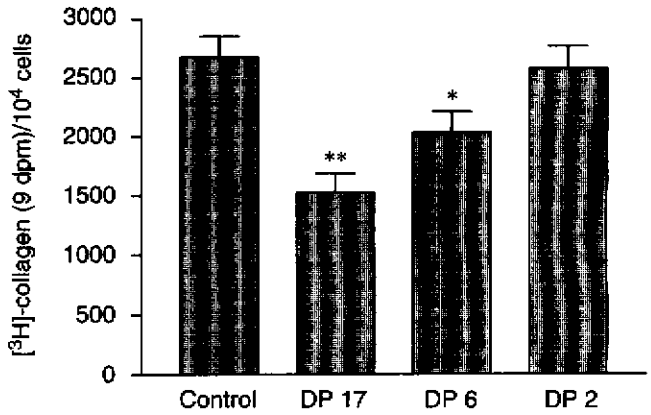

Fig. 4. Effect of DP (μg/mL) on total collagen production by HPMC. All values were normalized by cell number (10^4 cells). $*P < 0.05$ and $**P < 0.01$ relative to control. The experiment was repeated four times in triplicate.

drogenase (LDH) activity of the supernatant as we previously described [10, 11]. No differences were found in the numbers of dead cells in the supernatant and adherent HPMC fractions between control and DP-treated wells (data not shown).

Dipyridamole increased intracellular cAMP levels in HPMC

Dipyridamole is known to function as a phosphodiesterase inhibitor, thereby increasing intracellular cAMP levels [3, 5]. To evaluate whether DP increases intracellular cAMP levels in HPMC, we measured cAMP levels after incubation of HPMC with varying concentrations of DP (2, 6, and 17 μg/mL). In these experiments, IBMX (1 mmol), a known phosphodiesterase inhibitor, was used as a positive control (Fig. 3). cAMP levels were elevated in a dose-dependent manner by DP. The addition of DP at concentrations of 6 and 17 μg/mL resulted in a significant increase in the intracellular cAMP levels in HPMC. As expected, the addition of IBMX showed a significant increase in intracellular cAMP levels in HPMC.

Dipyridamole inhibited collagen synthesis of HPMC

As shown in Figure 4, total collagen synthesis by HPMC was inhibited by DP in a dose-dependent manner. Additionally, Northern blot analysis showed that DP decreased collagen α1 (I) and collagen α1 (III) mRNA levels (Fig. 5). The results of densitometry showed that, after 12 hours of incubation, DP decreased serum-stimulated collagen α1 (I) mRNA expression by 26% (collagen/GAPDH ratio 1.15 vs. 0.85 for lane 1 vs. 3). After 24 hours of incubation, DP decreased (collagen/GAPDH ratio 0.6 and 1.27 for lanes 4 and 5, respectively) collagen α1 (I) gene expression by 55% compared with that treated with serum alone. We have previously demonstrated a suppressive effect of collagen α1 (I) mRNA expression by DBcAMP (1 mmol) in cultured HPMC [11]. In our current study, the expression of collagen α1 (III) mRNA in HPMC was also suppressed after the addition of DBcAMP (1 mmol; data not shown).

In vivo studies

Gross adhesion scoring system. Figure 6 shows the results of the adhesion assessment in the different treatment groups. Group 1 (bacteria only) exhibited a mean score of 0.9 ± 0.18, which was not significantly different

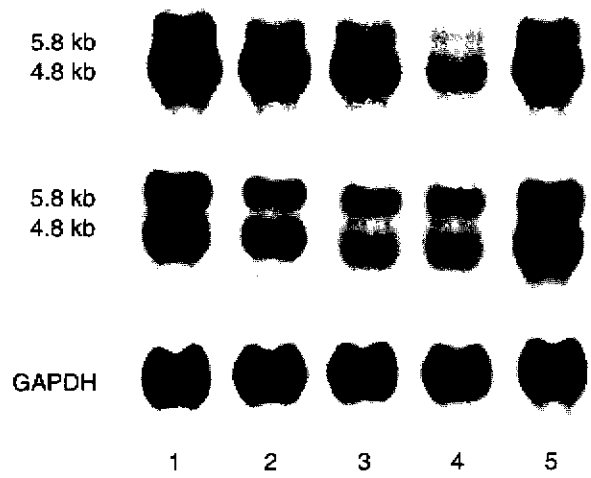

Fig. 5. Effects of DP on collagen α1 (I) and collagen α1 (III) mRNA levels. Lane 1, control at zero time; lanes 2–4, treatment of cells with DP (17 μg/mL) for 6 hours, 12 hours, and 24 hours, respectively; lane 5, control at 24 hours.

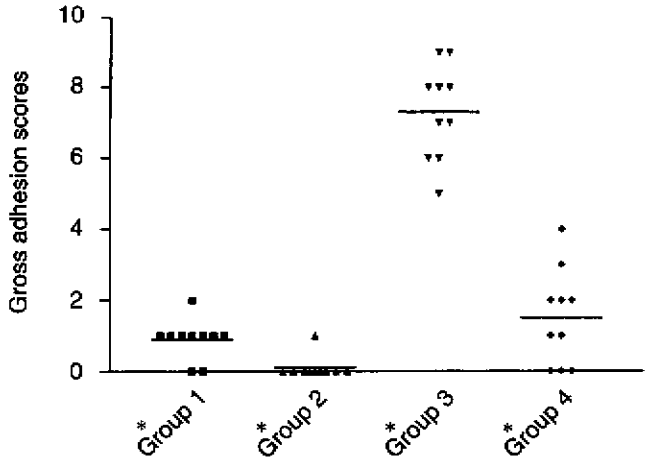

Fig. 6. Treatment of DP on adhesion formation in rats. The rat in group 3 (Cytodex mixed with bacteria) had the highest score (mean score 7.3 ± 0.42) of adhesion ranking, and the adhesion score was significantly reduced in rats treated with DP (group 4, mean score 1.5 ± 0.43). There was no significant difference between the group that received bacteria only (group 1) and the group that received Cytodex only (group 2); the means of the adhesion scores were 0.9 ± 0.18 and 0.1, respectively. *$P < 0.01$ compared to group 3.

from group 2 (Cytodex alone) with a mean score of 0.1. In contrast, the rats in group 3 (Cytodex and bacteria) had marked intraperitoneal adhesions with a mean adhesion score of 7.3 ± 0.42. Treatment with DP (group 4) resulted in a significant reduction of the adhesion score to a mean of 1.5 ± 0.43 ($P < 0.01$, compared to group 3). In this group, three (30%) rats were free of adhesions. There was no significant difference in gross visual adhesion scores between the control (saline only, data not shown) and group 1 or 2 rats.

Histological analysis. Figure 7 shows photomicrographs of representative sections taken from animals after treatment. Upon histologic examination, the normal peritoneum consists of a single layer of mesothelial cells and their underlying submesothelial tissue. In the histology specimen of rats treated with saline alone (control), no fibrosis was observed (not shown). In comparison to the control group, the fibrosis was much more prominent in group 3 rats, which had advanced gross intraperitoneal adhesions. An increased connective tissue deposit, which appeared as a thickening between the fragmented mesothelial layer of the peritoneum and the liver surface, was noted (Fig. 7C). The images in Figure 7 E–H are representative of different treatment groups showing the arteries of the gut mesentery. In group 3 rats (Fig. 7G), the walls of the small arteries appeared much thicker than those in the other three treatment groups; however, no increases were observed in wall thickness in small arteries of the gut mesentery in the DP treated rats (Fig. 7H). Figure 8 shows a comparison of the mean connective tissue thickness between the different treatment groups. Animals in groups 1 and 2 had the lowest mean value of peritoneal connective tissue thickness, whereas group 3 rats had the highest value. Treatment with bacteria plus Cytodex (group 3) triggered a fourfold increase in connective tissue thickness compared to the bacteria-treated (group 1) or Cytodex-treated rats (group 2; $P < 0.01$). Rats treated with DP (group 4) had a significantly reduced connective tissue thickness (0.43 ± 0.04) compared with that of group 3 rats (0.96 ± 0.05; $P < 0.05$). These measurements revealed quantitative differences between groups, a result that is similar to that obtained by using the gross visual adhesion scoring system (Fig. 6).

Northern blot analysis. Northern blot analysis was applied to detect collagen α1 (I)/α1 (III) mRNA transcripts in peritoneal samples obtained from the four groups. The message expressed was significantly increased in samples from group 3 rats (bacteria + Cytodex treated) compared to that of group 1 (bacteria treated) or group 2 (Cytodex treated; Fig. 9). In contrast, the expression of both genes in peritoneal tissue was suppressed by DP (group 4).

DISCUSSION

In vitro effects

This study demonstrated the inhibition of HPMC growth by DP (Figs. 2 and 3), an effect similar to what we previously reported in cultured rat mesangial cells [6]. DP also suppressed total collagen synthesis of HPMC in a dose-dependent manner (Fig. 5). By Northern blotting, the present study showed that DP attenuated the mRNA levels of collagen α1 (I) and collagen α1 (III) at 24 hours (Fig. 6). These in vitro effects of DP indicate that it has therapeutic potential for PF in vivo.

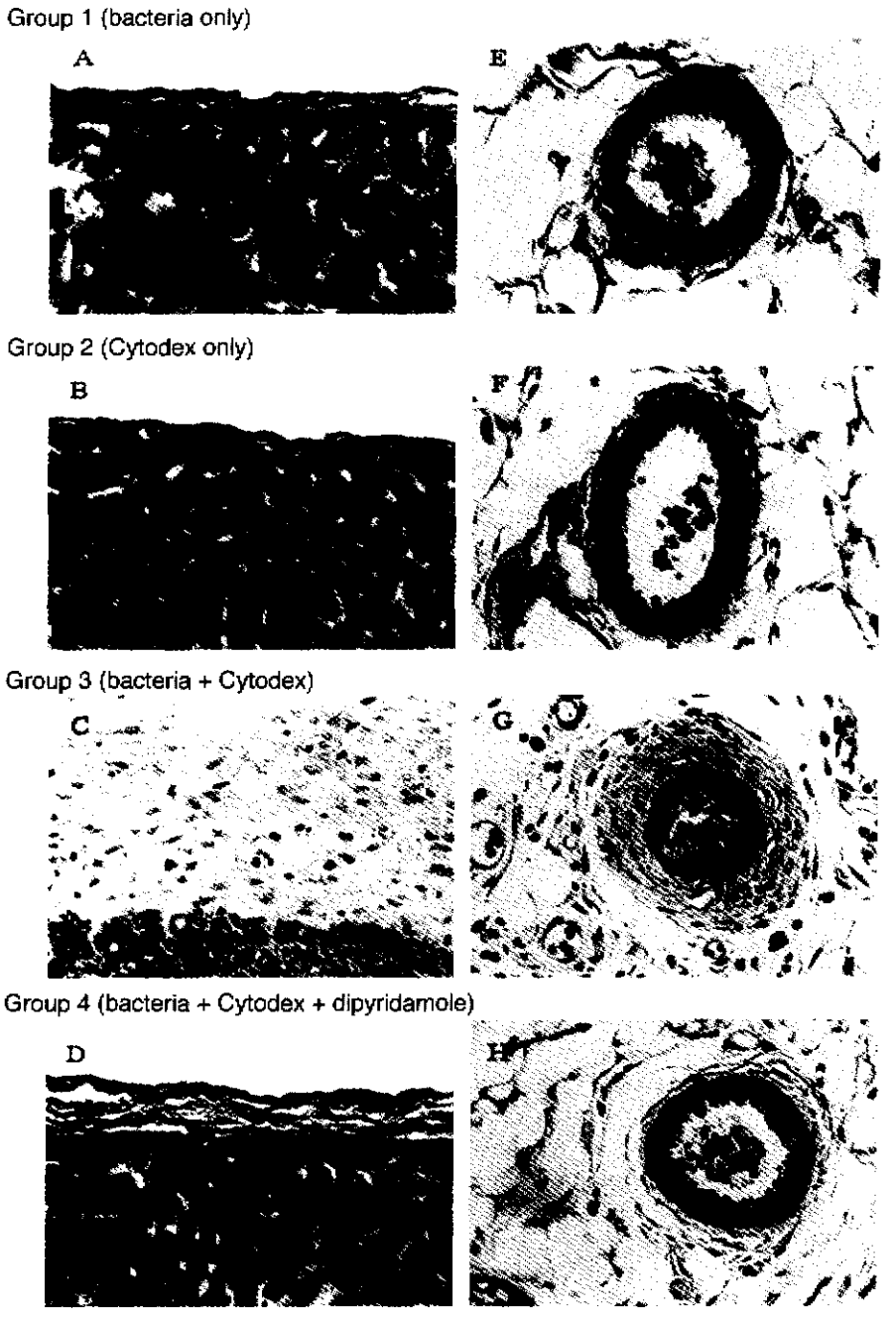

Fig. 7. Histological assessment of fibrotic reaction in peritoneal tissues. Representative sections of Trichrome-Masson-stained peritoneum displaying fibrotic thickening between the mesothelial layer and liver surface (*A–D*). Arteries of gut mesentery displaying different magnitudes of wall thickness attributable to fibrotic deposition in the four groups (*E–H*) (original magnification ×200).

It has been suggested that DP acts as an antiplatelet agent by serving as a phosphodiesterase inhibitor that increases intracellular cAMP [3, 5]. Our current study demonstrates an increase of intracellular cAMP after DP treatment (Fig. 4), while our previous reports showed that raised intracellular cAMP could inhibit serum-stimulated HPMC proliferation and collagen synthesis [11], and also demonstrated that N-[2-((p-Bromocinnamyl) amino)ethyl]-5-isoquinolinesulfonamide (H-89), a protein kinase A (PKA) inhibitor, could reverse the antimitogenic and antifibrogenic effects of a phosphodiesterase inhibitor (pentoxifylline) on HPMC [18]. These data combined indicate that the effect of DP may be through the cAMP pathway. The influence of cAMP on growth regulation of HPMC, with a focus on cell-cycle machinery such as cyclin D1 and $p27^{kip1}$, is currently being pursued in our laboratory. We found that the inhibitory effects of DP and cAMP on HPMC may be through the attenuated mitogen-activated protein kinase (MAPK) activity and alterations in expressions of $p27^{kip1}$ and retinoblastoma gene product (pRB) (unpublished data).

The development of PF resulted mainly from an over-

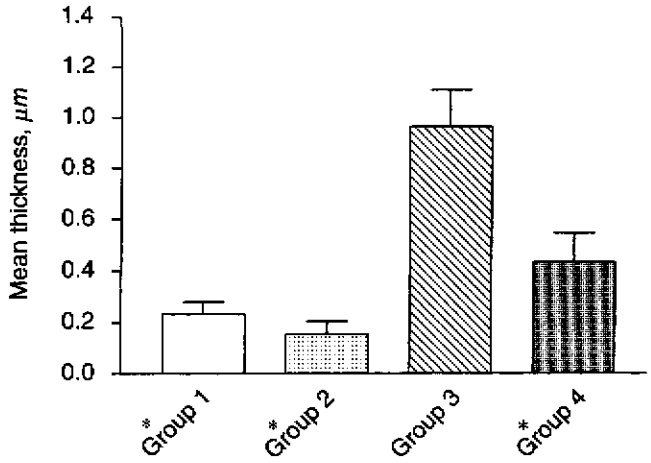

Fig. 8. Comparisons of connective tissue thickness (μm) between different groups. Thickness was assessed using Trichrome-Masson's stain (see **Methods** section). $^*P < 0.05$ compared to group 3.

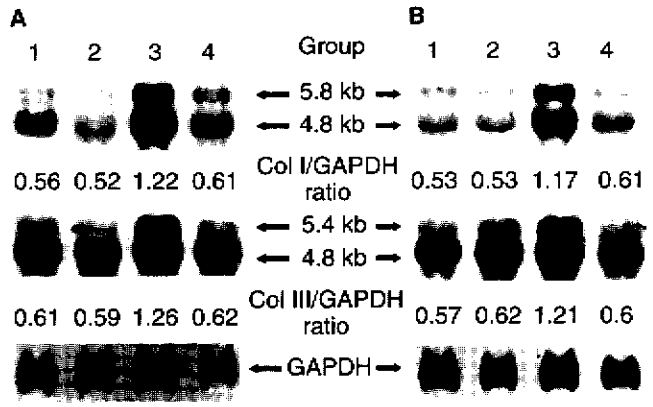

Fig. 9. Expression of collagen α1 (I) and collagen α1 (III) mRNA in adhesion strands of (*A*) omentum and (*B*) abdominal wall tissues. Shown are representative Northern blots performed as described in the **Methods** section. Both collagen α1 (I) and α1 (III) mRNA expressions were significantly increased in group 3 (rats treated with bacteria plus Cytodex). In contrast, the expression of both genes was suppressed by DP (group 4).

growth of mesothelial cells and/or the accumulation of extracellular matrix. The dual inhibitory effects of DP on HPMC proliferation and collagen synthesis, as demonstrated in our cell culture model, form the rationale for animal experiments to study DP therapy in PF induced subsequently to peritonitis.

In vivo effects

Histological findings of PF in the peritoneum obtained from patients [17] and experimental animals [19] are reportedly characterized by (*1*) impaired re-mesothelialization of the peritoneum; (*2*) increased fibro-connective tissue deposition resulting in thickening of the peritoneum and walls of small arteries in the gut mesentery; and (*3*) the possible prevalence of inflammatory infiltration. In our experiments, the degree of PF in rats treated with a mixed suspension of bacteria plus Cytodex (group 3) was prominent. Both gross development of peritoneal adhesions (Fig. 6) and connective tissue deposits (Figs. 7 and 8) were significantly increased. This group also demonstrated an increase in the mRNA levels of matrix components in peritoneal tissue samples (Fig. 9). In contrast, administration of DP to diseased rats seemed to provide remarkable protection and showed (*1*) an almost complete suppression of peritoneal adhesions (Fig. 6); (*2*) less thickness of connective tissue between the mesothelium and abdominal organs (Fig. 7 A–D and 8); (*3*) attenuation of increased wall thickness of small arteries (Fig. 7 E–H); and (*4*) a marked decrease in gene expression of collagen I and III in omentum and abdominal wall samples (Fig. 9).

There is no standard method for assessing the degree of peritoneal adhesion. Measurement of connective tissue thickness is the most common method for rating connective tissue deposition (fibrosis) [16]. Nevertheless, a gross visual scoring system may provide a quick and semiquantitative assessment of adhesion formation among treatment groups [15]. The present study used gross observation and grading of intraperitoneal changes (Fig. 6) as well as measurement of actual connective tissue thickness (Fig. 8) to show a suppressive effect of DP on adhesion formation. Furthermore, there was a good correlation between the gross observation scores and actual connective tissue thicknesses ($P < 0.01$, Pearson's method, data not shown). Our results suggest that the gross observation scoring system of Mullarniemi et al is convenient and as helpful as the method of actual measurement of connective tissue thickness in evaluating intraperitoneal fibrosis formation [15].

Peritonitis is the main culprit for CAPD patients to develop PF [20]. Experiments have shown that during peritonitis, if the peritoneal fibrinolytic process is not adequate, an ongoing fibrosis process will initiate, resulting in the possible development of adhesions between opposing peritoneal surfaces [21]. The functional fibrinolytic activity is decreased by the severity of peritonitis and existence of foreign bodies [22]. Cytodex has been used as a foreign material to promote local abscess formation in experimental mice [14]. Using this foreign substance, we successfully generated an easily observed and reproducible in vivo rat model of PF. The mechanisms by which Cytodex enhances PF development in our rat model are still not fully understood. Recently, in vitro studies have provided evidence of the importance of mesothelial cells for the balance of peritoneal procoagulant and fibrinolytic activity [23]. The roles of Cytodex and *S. aureus* on alterations in the balance of peritoneal procoagulant and fibrinolytic activity deserve further study.

Our rat model of PF may be somewhat remote from clinical situations in CAPD. However, given that peritonitis due to bacterial infection is one of the leading causes of the development of PF, the results obtained from our animal model may still have clinical implications. Our study represents only a first step for evaluating the effectiveness of this drug on PF in vivo. We did not perform a peritoneal transport assessment to evaluate peritoneal membrane function in the present work because of the following considerations: During peritonitis, peritoneal permeability is increased; however, as we found by gross inspection (Fig. 6), multiple intraperitoneal adhesions and fibrotic retractions may reduce peritoneal volume capacity. Therefore, in the present animal model it would have been difficult to tell whether the changes of peritoneal transport came from effects of peritoneal exchange volume or from peritoneal permeability. A chronic model (that is, one with a longer follow-up period) of the experimental animals and assessment of peritoneal membrane function may help to clarify the relationships between histological and functional changes of the peritoneum.

In conclusion, our study shows, to our knowledge for the first time, that in vitro DP effectively inhibits HPMC proliferation and decreases matrix accumulation. Moreover, it attenuates development of PF in vivo. These results suggest that DP may have potential therapeutic value for the prevention of PF in CAPD patients.

ACKNOWLEDGMENTS

This study was supported by grants from the National Science Council (NSC 89-2314-B-002-059), Ta-Tung Kidney Foundation, and Mrs. Hsiu-Chin Lee Kidney Research Fund, Taipei. The authors thank Ms. Chen-Chih Chang and Mr. Kuo-Tong Huang for their technical assistance.

Reprint requests to Dr. Tun-Jun Tsai, Department of Internal Medicine, National Taiwan University Hospital, No. 7, Chung-Shan South Road, Taipei, Taiwan, Republic of China.
E-mail: paul@ha.mc.ntu.edu.tw

APPENDIX

Abbreviations used in this article are: BHI, brain-heart infusion; BSA, bovine serum albumin; cAMP, cyclic adenosine 3'5'-monophosphate; CAPD, continuous ambulatory peritoneal dialysis; CFU, colony-forming unit; DP, dipyridamole; EIA, enzyme immunoassay; EDTA, ethylediaminetetraacetic acid; FCS, fetal calf serum; GADPH, glyceraldehyde-3-phosphate dehydrogenase; HPMC, human peritoneal mesothelial cells; H-89, N-[2-((p-Bromocinnamyl)amino)ethyl]-5-isoquinolinesulfonamide; IBMX, 3-isobutyl-1-methylxanthine; IM, intramuscular; IP, intraperitoneal; IVF, continuous intravenous infusion; LDH, lactate dehydrogenase; MAPK, mitogen-activated protein kinase; MTT, 3-[4,5-dimethylthiazol-2-yl]-2,5-diphenyltetrazolium bromide; PBS, phosphate-buffered saline; PF peritoneal fibrosis; PKA, protein kinase A; pRB, retinoblastoma gene product.

REFERENCES

1. Jacobs C: Current trends in dialysis therapy. *Kidney Int* 51(Suppl 62):S93–S95, 1997
2. Dobbie JW: Pathogenesis of peritoneal fibrosing syndrome (sclerosing peritonitis) in peritoneal dialysis. *Perit Dial Int* 12:14–27, 1992
3. Fitzgerald GA: Dipyridamole. *N Engl J Med* 316:1247–1257, 1987
4. Iimura O, Kusano E, Amemiya M, *et al:* Dipyridamole enhances interleukin-1β-stimulated nitric oxide production by cultured rat vascular smooth muscle cells. *Eur J Pharmacol* 296:319–326, 1996
5. Hillis GS, Duthie LA, MacLeod AM: Dipyridamole inhibits human mesangial cell proliferation. *Nephron* 78:172–178, 1998
6. Tsai TJ, Lin RH, Chang CC, *et al:* Vasodilator agents modulate rat glomerular mesangial cell growth and collagen synthesis. *Nephron* 70:91–100, 1995
7. Tzamaloukas AH: Peritonitis in peritoneal dialysis patients: An overview. *Adv Renal Replacement Ther* 3:232–236, 1996
8. Calame W, Afram C, Bluileven N, *et al:* Establishing an experimental infection model for peritoneal dialysis: Effect of inoculum and volume. *Perit Dial Int* 13(Suppl 2):S79–S80, 1993
9. Wieczorowska K, Khanna R, Moore HL, *et al:* Rat model of peritoneal fibrosis: Preliminary observations. *Adv Perit Dial* 11:48–51, 1995
10. Tsai TJ, Yen CJ, Fang CC, *et al:* Effect of intraperitoneally administered agents on human peritoneal mesothelial cell growth. *Nephron* 71:23–28, 1995
11. Fang CC, Yen CJ, Chen YM, *et al:* Hydralazine inhibits human peritoneal mesothelial cell proliferation and collagen synthesis. *Nephrol Dial Transplant* 11:2276–2281, 1996
12. Smith PK, Krohn RI, Hermanson GT, *et al:* Measurement of protein using bicinchoninic acid. *Anal Biochem* 150:76–85, 1985
13. Renvall S, Lehto M, Penttinen R: Development of peritoneal fibrosis occurs under the mesothelial cell layer. *J Surg Resear* 43:407–412, 1987
14. Ford CW, Hamel JC, Stapert D, Yancey RJ: Establishment of an experimental model of a *Staphylococcus aureus* abscess in mice by use of dextran and gelatin microcarriers. *J Med Microbiol* 28:259–266, 1988
15. Mullarniemi H, Frilander M, Turunen M, Saxen L: The effect of glove powders and their constituents on adhesion and granuloma formation in the abdominal cavity of the rabbit. *Acta Chir Scand* 131:312–317, 1966
16. Frazier-Jessen MR, Kovacs E: Abdominal wall thickness as a means of assessing peritoneal fibrosis in mice. *J Immunol Method* 162:115–121, 1993
17. Nakamoto M: Pathogenesis of peritoneal fibrosis and peritoneal small vessel changes. *Perit Dial Int* 16(Suppl 1):S39–S41, 1996
18. Fang CC, Yen CJ, Chen YM, *et al:* Pentoxifylline inhibits human peritoneal mesothelial cell growth and collagen synthesis: Effects on TGF-β. *Kidney Int* 57:2626–2633, 2000
19. Fracasso A, Baggio B, Ossi E, *et al:* Glycosaminoglycans prevent the functional and morphological peritoneal derangement in an experimental model of PF. *Am J Kidney Dis* 33:105–110, 1999
20. Rottembourg J, Issad B, Langlois P: Sclerosing encapsulating peritonitis during CAPD. Evaluation of the potential risk factors, in *Frontiers in Peritoneal Dialysis*, edited by Maher JF, Winchester JF, New York, Field, Rich and Assoc., Inc., 1986, pp 643–649
21. diZerega GS: Biochemical events in peritoneal tissue repair. *Eur J Surg* 163(Suppl 577):10–16, 1997
22. Holtz G: Prevention and management of peritoneal adhesions. *Fertil Steril* 41:497–507, 1984
23. Sitter T, Spannagl M, Schiffl H, *et al:* Imbalance between intraperitoneal coagulation and fibrinolysis during peritonitis of CAPD patients: The role of mesothelial cells. *Nephrol Dial Transplant* 10:677–683, 1995